CERN-EP-2021-158
2022/07/18

CMS-B2G-20-008

Search for heavy resonances decaying to $Z(\nu\overline{\nu})V(q\overline{q}')$ in proton-proton collisions at $\sqrt{s} = 13\,\text{TeV}$

The CMS Collaboration*

Abstract

A search is presented for heavy bosons decaying to $Z(\nu\overline{\nu})V(q\overline{q}')$, where V can be a W or a Z boson. A sample of proton-proton collision data at $\sqrt{s} = 13\,\text{TeV}$ was collected by the CMS experiment during 2016–2018. The data correspond to an integrated luminosity of $137\,\text{fb}^{-1}$. The event categorization is based on the presence of high-momentum jets in the forward region to identify production through weak vector boson fusion. Additional categorization uses jet substructure techniques and the presence of large missing transverse momentum to identify W and Z bosons decaying to quarks and neutrinos, respectively. The dominant standard model backgrounds are estimated using data taken from control regions. The results are interpreted in terms of radion, W′ boson, and graviton models, under the assumption that these bosons are produced via gluon-gluon fusion, Drell–Yan, or weak vector boson fusion processes. No evidence is found for physics beyond the standard model. Upper limits are set at 95% confidence level on various types of hypothetical new bosons. Observed (expected) exclusion limits on the masses of these bosons range from 1.2 to 4.0 (1.1 to 3.7) TeV.

Published in Physical Review D as `doi:10.1103/PhysRevD.106.012004`.

*See Appendix A for the list of collaboration members

1 Introduction

The search for physics beyond the standard model (SM) using proton-proton (pp) collisions produced by the CERN LHC is a key goal of the CMS physics program. The apparent large hierarchy between the electroweak scale and the Planck scale, the nature of dark matter, and the possibility of a unification of the gauge couplings at high energies, are among the outstanding problems in particle physics not addressed within the SM. New bosons are predicted in many beyond-the-SM theories, which attempt to answer some of these questions. New spin-0 and spin-2 particles are predicted in the Randall–Sundrum (RS) models of warped extra dimensions [1, 2], which arise from radion and graviton fields. Spin-1 W' and Z' bosons can also arise in these models [3–5], as well as in left-right symmetric theories [6], and little Higgs models [7–9]. When the interaction strength between a new boson and the SM boson field is large, such as in the bulk RS models [10, 11], searches for diboson resonances are motivated, either via weak vector boson fusion (VBF) or strong production processes.

This paper presents a search for new bosons (X) decaying either to a pair of Z bosons or to a W and a Z boson, as shown in Fig. 1. In addition to VBF production, we consider gluon-gluon fusion (ggF) production of spin-0 and spin-2 particles, and Drell–Yan (DY) production of spin-1 particles. The targeted final state is one in which one Z boson decays into a neutrino pair, while the other vector boson decays hadronically into jets. Searches for similar signatures have been presented by the ATLAS [12] and CMS [13] Collaborations with the LHC data recorded in 2015 and 2016. Compared to earlier CMS publications, this paper includes additional data, new interpretations in terms of radion models, and extends the analysis to new search regions by including event categories that identify forward jets consistent with VBF production. An analysis similar to the one presented here was published by the ATLAS Collaboration using data recorded in 2015–2018 [14]. In that analysis, no significant deviations from the SM were observed.

In the present work, proton-proton collisions at $\sqrt{s} = 13\,\text{TeV}$ recorded during 2016–2018 with the CMS detector are analyzed. The data set corresponds to an integrated luminosity of $137\,\text{fb}^{-1}$. Events are selected that have a high-mass jet and a significant amount of missing transverse momentum ($p_{\mathrm{T}}^{\text{miss}}$), which is the signature of the $\mathrm{Z} \to \nu\overline{\nu}$ decay. Events are categorized by the presence or absence of jets at large pseudorapidity (forward jets). Events that include forward jets are typical of VBF production. Events without forward jets more commonly occur in ggF or DY processes. For sufficiently heavy new bosonic states, the decaying vector bosons will have high momenta and, when decaying hadronically, will appear in the detector as single jets. As a result, we employ jet substructure techniques to identify these objects. Contributions from the dominant backgrounds are determined using control samples in data.

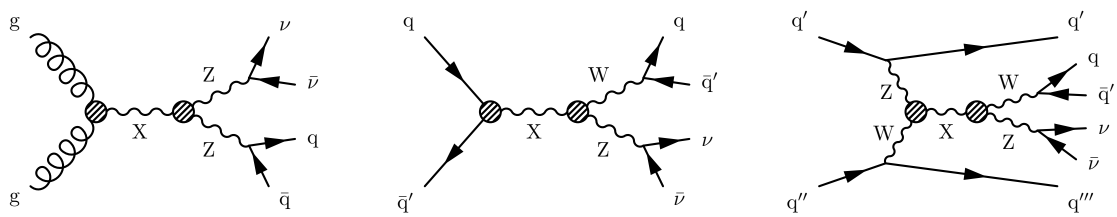

Figure 1: Representative Feynman diagrams for various production modes of a heavy resonance X. These modes are: a ggF-produced spin-0 or spin-2 resonance decaying to $\mathrm{ZZ} \to \mathrm{q\overline{q}}\nu\overline{\nu}$ (left), a DY-produced spin-1 resonance decaying to $\mathrm{WZ} \to \mathrm{q\overline{q}'}\nu\overline{\nu}$ (center), and a VBF-produced spin-1 resonance decaying to $\mathrm{WZ} \to \mathrm{q\overline{q}'}\nu\overline{\nu}$ (right).

This paper is organized as follows. Section 2 gives a brief description of the CMS detector and its components relevant to this work. Section 3 summarizes the simulated data sets used in this analysis. Algorithms for the reconstruction of physics objects and the selection criteria applied to these objects are described in Sections 4 and 5, respectively. Section 6 discusses methods used for estimating the SM backgrounds. The systematic uncertainties relevant to this analysis are described in Section 7. The final results are presented in Section 8, along with their statistical interpretations. A summary of the work is presented in Section 9. Tabulated results are provided in the HEPData record [15] for this analysis.

2 The CMS detector

The central feature of the CMS detector is a superconducting solenoid of 6 m internal diameter, providing a magnetic field of 3.8 T. Within the solenoid volume are a silicon pixel and strip tracker, a lead tungstate crystal electromagnetic calorimeter, and a brass and scintillator hadron calorimeter. Each of these systems is composed of a barrel and two endcap sections. The tracking detectors cover the pseudorapidity range $|\eta| < 2.5$. For the electromagnetic and hadronic calorimeters, the barrel and endcap detectors together cover the range $|\eta| < 3.0$. Forward calorimeters extend the coverage to $|\eta| < 5.0$. Muons are measured and identified in both barrel and endcap systems, which together cover the pseudorapidity range $|\eta| < 2.4$. The detection planes are based on three technologies: drift tubes, cathode strip chambers, and resistive-plate chambers, which are embedded in the steel flux-return yoke outside the solenoid. The detector is nearly hermetic, permitting accurate measurements of $p_{\mathrm{T}}^{\mathrm{miss}}$. Events of interest are selected using a two-tiered trigger system [16, 17]. The first level, composed of custom hardware processors, uses information from the calorimeters and muon detectors to select events at a rate of around 100 kHz within a fixed time interval of less than 4 μs. The second level, known as the high-level trigger, consists of a farm of processors running a version of the full event reconstruction software optimized for fast processing, and reduces the event rate to around 1 kHz before data storage. A more detailed description of the CMS detector, together with a definition of the coordinate system used and the relevant kinematic variables, can be found in Ref. [18].

3 Simulated event samples

This search uses Monte Carlo (MC) simulated data sets to study and guide the estimations of SM background processes. Simulated data sets include: V+jets, where V refers to W or Z bosons, $\mathrm{t\bar{t}}$+jets, single top quark samples, diboson and triboson samples (WZ, WZZ, etc.), and $\mathrm{t\bar{t}}$+V samples. Events in these samples for 2016 (2017 and 2018) are generated using MADGRAPH5_aMC@NLO v2.2.2 (v2.4.2) [19–22]. The V+jets ($\mathrm{t\bar{t}}$+jets) samples are generated with leading order (LO) precision in the perturbative expansion of quantum chromodynamics (pQCD) and contain up to four (three) additional partons in the matrix element calculations. The t-channel and tW single top quark events, and WW events for 2016 (2017 and 2018) are generated using POWHEG v1.0 (v2.0) [23–27] at next-to-LO (NLO) precision in pQCD. All other SM background samples are generated using MADGRAPH5_aMC@NLO at NLO precision in pQCD. The signal samples used for interpretation of the results are also generated using MADGRAPH5_aMC@NLO with LO precision in pQCD.

The parton showering and hadronization step in all simulations is performed with two versions of PYTHIA [28]. The 2016 (2017 and 2018) simulation uses the CUETP8M1 [29] (CP5 [30]) underlying event tune with PYTHIA v8.212 (v8.230). The parton distribution functions (PDFs) used in the 2016 (2017 and 2018) simulated data samples are NNPDF3.0 LO or NLO [31] (NNPDF3.1

NNLO [32]). The simulation of the particle interactions and the CMS detector is performed with GEANT4 [33]. The effects due to additional pp interactions in the same or adjacent bunch crossings (pileup) are also simulated and the events are weighted to match the pileup distribution in data.

The cross sections used to normalize different SM processes correspond to NLO or next-to-NLO (NNLO) accuracy [19, 26, 27, 34–42]. The V+jets samples are weighted based on the transverse momentum (p_{T}) of the W and Z bosons. Weights are derived from comparisons of LO simulations and simulations at NNLO precision in pQCD interactions and NLO precision in electroweak interactions [43].

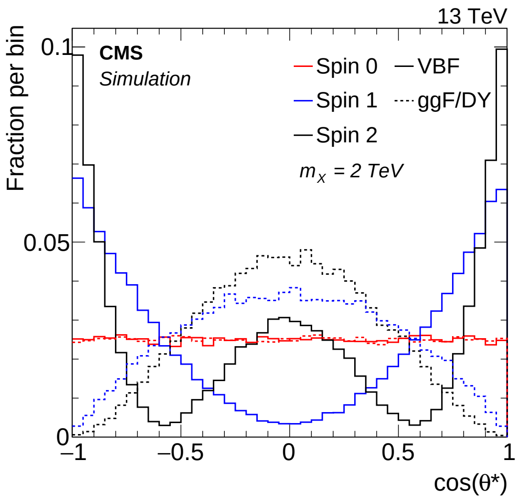

Figure 2: Simulated distributions are shown for the cosine of the decay angle of SM vector bosons in the rest frame of a parent particle with a mass (m_{X}) of 2 TeV. Solid lines represent VBF scenarios. Dashed lines represent ggF/DY scenarios. The integral of each histogram is normalized to unity.

When diboson signatures are produced through VBF, correlations between the spin of initial- and final-state bosons cause event kinematic distributions to depend on the hypothesized resonance spin. These correlations are manifested in the decay angle, θ^*, of the vector bosons, defined in Ref. [44]. Figure 2 shows the distribution of the cosine of the decay angles in the rest frame of X for each spin configuration and production mechanism we consider, given a parent particle mass of 2 TeV. Scalar resonances have no correlation between initial- and final-state spins, which translates to a flat $\cos\theta^*$ distribution. Spin-1 and spin-2 particles can have strong correlations, especially when produced via VBF, where vector bosons are preferentially produced in the forward direction ($\cos\theta^* \simeq \pm1$). Such correlations are caused by the production of longitudinally or transversely polarized vector bosons [45]. The decay angle is correlated with the p_{T} of the resonance's decay products. Thus, the spectral features explored here are different from typical diboson searches because the final state is only partially reconstructed. We explore the sensitivity of the analysis to the assumed spin by considering three different production models: radions (spin 0), W′ bosons (spin 1), and gravitons (spin 2). In each case, we consider both VBF and ggF or DY production, and masses between 1.0 and 4.5 TeV in steps of 200 (500) GeV for masses less (greater) than 2.0 TeV.

To interpret the data in terms of spin-0 and spin-2 signals, radions and gravitons arising from models of warped extra dimensions [1, 2], and specifically from bulk scenarios [10, 11], are used as representative models. The warped extra dimension model has several free parameters, including the mass of the lowest excited state of the graviton, the radion mass, the parameter

$kr_c\pi$, where k and r_c are the curvature and the compactification scale of the extra dimension respectively, the dimensionless coupling $\widetilde{k} = k/\overline{M_{\rm Pl}}$, where $\overline{M_{\rm Pl}}$ is the reduced Planck mass, and the energy scale associated with radion interactions ($\Lambda_{\rm R}$). These parameters and the corresponding cross sections are described in Ref. [45]. We assume $\widetilde{k} = 0.5$, $kr_c\pi = 35$, and $\Lambda_{\rm R} = 3\,\text{TeV}$, which results in decay widths for gravitons and radions smaller than 10% of their mass. The predicted cross sections for radions and gravitons produced via ggF (VBF) are accurate to NLO (LO) in pQCD.

To interpret data in terms of spin-1 signals, $\rm W'$ bosons within the heavy vector triplet (HVT) framework [6] are used. The interactions between $\rm W'$ bosons and SM particles are parameterized in terms of $c_{\rm H}$, $g_{\rm V}$, and $c_{\rm F}$ couplings and the mass of the HVT $\rm W'$ boson. Together with the SM $\rm SU(2)_L$ gauge coupling, g, these parameters determine the couplings between the HVT bosons and the SM Higgs boson, SM vector bosons, and SM fermions, respectively, according to Ref. [6]. We consider two specific cases of these model parameters: those corresponding to model B ($c_{\rm H} = -0.98$, $g_{\rm V} = 3$, and $c_{\rm F} = 1.02$) in Ref. [6] and model C ($c_{\rm H} = g_{\rm V} = 1$ and $c_{\rm F} = 0$). Model B suppresses the fermion couplings, enhancing decays to SM vector bosons. Model C removes direct couplings to fermions, ensuring that only VBF production is possible. The predicted cross sections for $\rm W'$ bosons are accurate to LO in pQCD.

4 Triggers and event reconstruction

Samples of collision data are selected using several $p_{\rm T}^{\rm miss}$ triggers whose thresholds vary between 90 and 140 GeV, depending on the data-taking period. The $p_{\rm T}^{\rm miss}$ trigger efficiencies were studied using samples of events selected with single-lepton triggers. The lepton triggers isolate events with neutrinos produced via W boson decays, which serve as a good proxy for both the signal and the dominant backgrounds. The single-lepton triggers required electrons with $p_{\rm T} > 27$–$32\,\text{GeV}$, depending on the data-taking period, or muons with $p_{\rm T} > 24\,\text{GeV}$. The efficiencies of the triggers for selecting events with large $p_{\rm T}^{\rm miss}$ ($>$200 GeV) were measured as functions of $p_{\rm T}^{\rm miss}$. The differences between the efficiencies determined using electron events and muon events were found to be less than 1.4% and are assigned as systematic uncertainties. For all data-taking periods, the trigger efficiency is found to reach 95% for $p_{\rm T}^{\rm miss} > 250\,\text{GeV}$ and plateaus around 98% for $p_{\rm T}^{\rm miss} > 300\,\text{GeV}$. At $p_{\rm T}^{\rm miss} = 200\,\text{GeV}$, the efficiency is found to be greater than 75%. The trigger efficiencies measured using single-lepton data are applied to the simulated data as functions of the reconstructed $p_{\rm T}^{\rm miss}$. The dependence of these efficiencies on other kinematic variables has been investigated and the associated effects found to be less than the assigned uncertainties.

The event reconstruction proceeds from particles identified by the particle-flow (PF) algorithm [46], which uses information from the silicon tracking system, calorimeters, and muon systems to reconstruct PF candidates as electrons, muons, charged or neutral hadrons, or photons. The candidate vertex with the largest value of summed physics-object $p_{\rm T}^2$ is taken to be the primary pp interaction vertex. The physics objects used for this determination are jets, formed by clustering tracks assigned to candidate vertices using the anti-$k_{\rm T}$ jet finding algorithm [47, 48] with a distance parameter of 0.4, and the associated $\vec{p}_{\rm T}^{\rm miss}$, taken as the negative vector $p_{\rm T}$ sum of those jets.

Electrons are reconstructed by associating a charged-particle track with an electromagnetic calorimeter supercluster [49]. The resulting electron candidates are required to have $p_{\rm T} > 10\,\text{GeV}$ and $|\eta| < 2.5$, and to satisfy identification criteria designed to reject light-parton jets, photon conversions, and electrons produced in the decays of heavy-flavor hadrons. Muons are reconstructed by associating tracks in the muon system with those found in the silicon tracker [50]. Muon candidates are required to satisfy $p_{\mathrm{T}} > 10\,\mathrm{GeV}$ and $|\eta| < 2.4$.

Leptons (e, μ) are required to be isolated from other PF candidates to select preferentially those originating from W and Z boson decays and suppress backgrounds in which leptons are produced in the decays of hadrons containing heavy quarks. Isolation is quantified using an optimized version of the mini-isolation variable originally introduced in Ref. [51]. The isolation variable, I_{mini}, is calculated by summing the p_{T} of the charged and neutral hadrons, and photons with $\Delta R \equiv \sqrt{(\Delta\phi)^2 + (\Delta\eta)^2} < R_0$ of the lepton momentum vector, $\vec{p}^{\,\ell}$, where ϕ is the azimuthal angle and R_0 depends on the lepton p_{T}. The three values of R_0 used are: 0.2 for $p_{\mathrm{T}}^{\ell} \leq 50\,\mathrm{GeV}$; $(10\,\mathrm{GeV})/p_{\mathrm{T}}^{\ell}$ for $50 < p_{\mathrm{T}}^{\ell} < 200\,\mathrm{GeV}$; and 0.05 for $p_{\mathrm{T}}^{\ell} \geq 200\,\mathrm{GeV}$. Electrons (muons) are then required to satisfy $I_{\mathrm{mini}}/p_{\mathrm{T}}^{\ell} < 0.1\,(0.2)$. In order to mitigate the effects from pileup in an event, charged hadron candidates are required to originate from the primary vertex of the given event.

Events are vetoed in which muon or electron candidates are identified that satisfy isolated track requirements, $|\eta| < 2.4$, and $p_{\mathrm{T}} > 5\,\mathrm{GeV}$, but do not satisfy the kinematic requirements just described for isolated leptons. Hadronically decaying τ leptons can produce isolated hadron tracks. Events in which an isolated hadron track is identified that satisfies $|\eta| < 2.4$ and $p_{\mathrm{T}} > 10\,\mathrm{GeV}$ are also vetoed.

Events with one or more photons are vetoed. Photon candidates are required to have $p_{\mathrm{T}} > 100\,\mathrm{GeV}$, $|\eta| < 2.4$, and be isolated from neutral hadrons, charged hadrons, and electromagnetic particles, excluding the photon candidate itself. The isolation criterion is calculated using a cone with $\Delta R < 0.2$ around the photon [52].

Jets are reconstructed by clustering charged and neutral PF candidates using the anti-k_{T} algorithm. Two collections of jets are considered clustered with distance parameters $R = 0.4$ and 0.8, as implemented in the FASTJET package [48]. Depending on the distance parameter used, these jets are referred to as AK4 and AK8 jets, respectively. Jet energies are corrected using a p_{T}- and η-dependent jet energy calibration [53]. To mitigate contributions to jet reconstruction from pileup, we utilize the charged-hadron subtraction method for AK4 jets and the pileup-per-particle identification (PUPPI) method [54, 55] for AK8 jets.

Jets are required to satisfy $p_{\mathrm{T}} > 30\,(200)\,\mathrm{GeV}$, $|\eta| < 5.0\,(2.4)$, and jet quality criteria [56, 57] for AK4 (AK8) jets. The mass of AK8 jets and information about the pattern of energy deposited in various detectors are used to reconstruct massive vector bosons. To further reduce the dependence on pileup and to help reduce the effect of wide-angle soft radiation, the soft-drop algorithm [58, 59] is used to remove constituents from the AK8 jets. Corrections are applied to AK8 jets to ensure that the reconstructed jet mass reproduces the pole masses of the SM bosons. Corrections are derived using W bosons from $\mathrm{t\bar{t}}$ production to account for known differences between measured and simulated jet mass scale and jet mass resolution [60]. Finally, jets having PF constituents matched to an isolated lepton are removed from the jet collection.

The N-subjettiness [61] technique is used to distinguish between AK8 jets originating from the hadronic decay of W or Z bosons and those originating from quantum chromodynamics (QCD). In hadronic boson decays, the resulting jet is likely to have two substructure components, which results in a smaller N-subjettiness ratio, τ_{21}. For QCD jets, τ_{21} tends to be higher. We require AK8 jets to satisfy $\tau_{21} < 0.75$. There is a loss of about 36% in background events due to this requirement. Negligible loss of efficiency is observed due to this requirement in a signal sample of VBF-produced gravitons (VBFG) with a mass of 1 TeV. The efficiency for tagging W bosons in simulated data sets is validated against collision data using $\mathrm{t\bar{t}}$ events [60]. Scale factors are applied to simulated data sets to account for observed differences.

The AK4 jets are tagged as originating from the hadronization of b quarks using the deep combined secondary vertex algorithm [62]. For the medium working point chosen here, the signal efficiency for identifying b jets with $p_T > 30$ GeV in $t\bar{t}$ events is about 68%. The probability of misidentifying jets in $t\bar{t}$ events arising from c quarks is approximately 12%, while the probability of misidentifying jets associated with light-flavor quarks or gluons as b jets is approximately 1%.

The vector $\vec{p}_T^{\text{miss}}$ is defined as the negative vector p_T sum of all PF candidates and is calibrated taking into account the jet energy corrections. Its magnitude is denoted by p_T^{miss}. Dedicated event filters designed to reject instrumental noise are applied to improve the correspondence between the reconstructed and the genuine p_T^{miss} [63]. To suppress SM backgrounds, we use the quantity m_T, defined as the transverse mass of the system consisting of the highest p_T AK8 jet (p_T^J) and $\vec{p}_T^{\text{miss}}$. The value of m_T is computed as

$$m_T = \sqrt{2 p_T^J p_T^{\text{miss}} [1 - \cos \Delta\Phi]}, \tag{1}$$

where $\Delta\Phi$ is the difference between the azimuthal angle of the AK8 jet's momentum and $\vec{p}_T^{\text{miss}}$. The m_T variable in Eq. 1 assumes that the new state decays into much lighter daughter particles.

5 Event selection

The reconstructed objects (defined in Section 4) are used to define signal regions (SRs) and control regions (CRs). These are all subsets of a baseline phase space where at least one AK8 jet and $p_T^{\text{miss}} > 200$ GeV are required. Events are rejected if they contain a reconstructed electron, muon, photon, isolated track, or an AK4 jet which has been identified as a b jet. Events are vetoed if any jet passes the p_T and η requirements, but fails the jet quality criteria. Events are also vetoed if $\vec{p}_T^{\text{miss}}$ is aligned with the transverse projection of any of the four highest p_T AK4 jets, defined as $\Delta\phi(j_i, p_T^{\text{miss}}) < 0.5$.

The baseline phase space is split into two sets of regions, VBF and ggF/DY. The VBF regions require at least two AK4 jets, each required to be separated by $\Delta R > 0.8$ from the AK8 jet. The two highest-p_T AK4 jets are also required to be reconstructed in opposite hemispheres ($\eta_1\eta_2 < 0$), have a large pseudorapidity separation ($\Delta\eta > 4.0$), and form a large invariant mass ($m_{jj} > 500$ GeV). These requirements are indicative of VBF production. If any of these conditions is failed, the event is put into the ggF/DY category.

Both the VBF and ggF/DY categories are further separated into high-purity (HP) and low-purity (LP) categories, depending on the highest p_T AK8 jet's value of τ_{21}. Events in which the highest p_T AK8 jet satisfies $\tau_{21} < 0.35$ ($0.35 < \tau_{21} < 0.75$) are referred to as HP (LP). The signal (VBFG 1 TeV) selection efficiency with the high (low) purity cut is 69 (31)%. The background selection efficiency with the high (low) purity cut is 32 (68)%.

Each of these four event categories is divided into a number of m_T bins. Starting from $m_T = 400$ GeV, each bin has a width of 100 GeV. In the ggF/DY (VBF) HP category, the bin width is constant up to 2200 (1600) GeV, beyond which, bin boundaries correspond to $m_T = 2200$, 2350, 2550, 2750, and 3000 (1600, 1750, and 2075) GeV. In the ggF/DY (VBF) LP category, the bin width is constant up to 2900 (2300) GeV, beyond which bin widths are 200 GeV up to $m_T = 3500$ (2700) GeV. The last bin in each of the categories includes all events with m_T above the final quoted bin boundary.

In all m_T bins, an SR and a CR is defined based on the mass of the highest p_T AK8 jet, m_J. The SRs require $65 < m_J < 105$ GeV, a range which is chosen to accept both W and Z bosons, but reject most hadronically decaying Higgs bosons. The CRs require either $30 < m_J < 65$ GeV or $135 < m_J < 300$ GeV, which excludes the SR mass requirement and a window around the Higgs boson mass. The event selections used in the analysis are summarized in Table 1.

Table 1: Summary of the event selections.

Variable	Selection
p_T^{miss}	>200 GeV
Veto	electrons, muons, tau leptons, photons, b jets
AK4 jet p_T	>30 GeV
$\Delta\phi(\vec{p}_T^{jets}, \vec{p}_T^{miss})$	>0.5
Leading AK8 jet p_T and η	>200 GeV and $\|\eta\| < 2.4$
Leading AK8 jet mass	SR: 65–105 GeV, CR: 30–65 GeV or 135–300 GeV
τ_{21}	HP: <0.35, LP: 0.35–0.75
Forward jets	$(\eta_1\eta_2) < 0$, $\Delta\eta > 4.0$, $m_{jj} > 500$ GeV

The dominant backgrounds are events originating from W+jets and Z+jets production, followed by the $W \to \ell\nu$ and $Z \to \nu\bar{\nu}$ decays. In these events the charged leptons do not pass the reconstruction requirements described in Section 4, while the neutrinos manifest themselves as p_T^{miss}. In addition, the massive jets in these events do not arise from hadronically-decaying vector bosons; rather they arise from the tail of a smoothly falling distribution of jet mass. We refer to these and other processes with similar kinematic properties as nonresonant backgrounds. The shape and normalization of nonresonant backgrounds are constrained using data, as described in Section 6.

Subdominant SM contributions come from $t\bar{t}$, single top quark, and diboson processes. These processes typically have a hadronically-decaying vector boson. There is a small contribution from the diboson events produced via the vector boson scattering process. These events are expected to contribute less than 10% of the total diboson event yield in the VBF SRs. The contributions from subdominant backgrounds, referred to as resonant backgrounds, are estimated using predictions from simulation.

The reconstructed m_T distribution for the signal depends on the spin, mass, and production mechanism. Using events from all signal regions and control regions combined, Fig. 3 shows the m_T distributions for the various signal hypotheses considered. These distributions for VBF-produced W′ and graviton resonances are a reflection of the prevalence for vector bosons production at large η due to correlations between η and $\cos\theta^*$. When vector bosons have large η, the AK8 jet p_T and the p_T^{miss} are lower, and in turn, the reconstructed m_T is lower. For models with multimodal $\cos\theta^*$ distributions, there is a corresponding distortion in the m_T distribution, which tends to produce higher yields at lower values of m_T.

6 Background estimation method

The nonresonant backgrounds populate both the CRs and the SRs, while signal events mainly populate the SRs. The yields observed in the CRs are weighted by a transfer factor, α, to account for known differences between the SR and CR kinematic properties. The transfer factor is derived from simulated data sets. Algebraically, the predictions of the nonresonant backgrounds

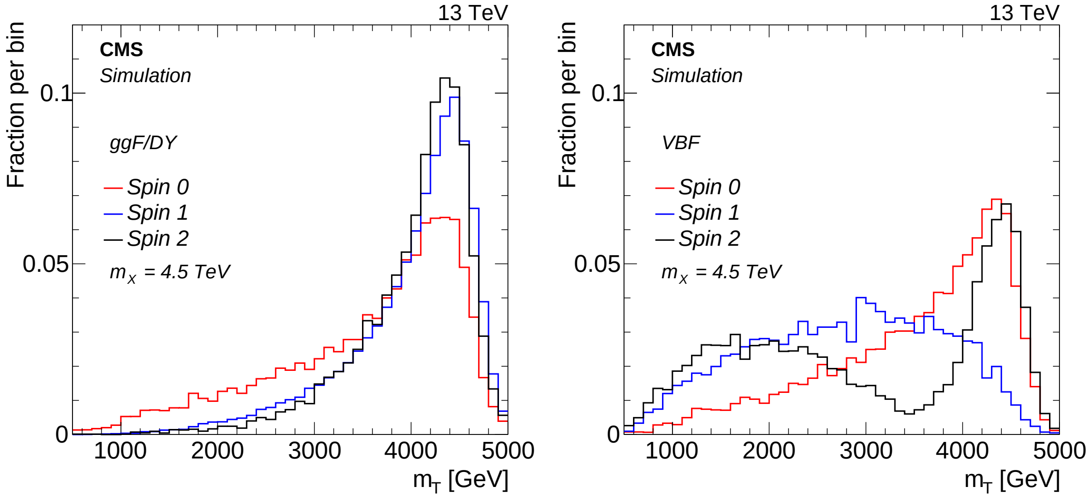

Figure 3: Distributions of m_{T} for ggF/DY- (left) and VBF-produced (right) resonances X of mass 4.5 TeV. Events used are from all SR and CR combined. The integral of each histogram is normalized to unity.

are given by

$$N_{\mathrm{pred}}^{\text{non-res}} = \alpha (N_{\mathrm{CR}}^{\mathrm{obs}} - N_{\mathrm{CR}}^{\mathrm{res}}),$$
$$\alpha = \frac{N_{\mathrm{SR}}^{\text{non-res}}}{N_{\mathrm{CR}}^{\text{non-res}}}, \tag{2}$$

where $N_{\mathrm{CR}}^{\mathrm{obs}}$ refers to the observed CR yields, and $N^{\text{non-res}}$ (N^{res}) refers to the nonresonant (resonant) background yields in simulated data sets. In this formula, N_{*}^{res} serves the role of removing the expected contributions from resonant backgrounds, which have a systematically different transfer factor and whose predictions are handled separately. All event yields are derived separately for each m_{T} bin and each event category. Figure 4 shows α as a function of m_{T} in each of the event categories.

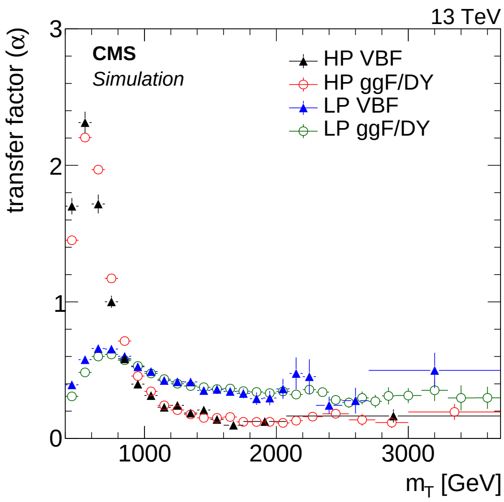

Figure 4: The distributions of the transfer factors (α) versus m_{T} in the various event categories are shown. The last bin corresponds to the value obtained by integrating events above the penultimate bin.

The resonant backgrounds are directly estimated using predictions from simulation, with systematic uncertainties evaluated to account for potential data mismodeling. The resonant background yields are used to account for contamination in the CRs before predicting the nonresonant backgrounds and their contribution to the SRs themselves.

The procedures used to predict SM backgrounds have been validated using data from a subset of each CR, which we refer to as the validation SR (vSR). The vSRs have the same selections as the SRs except that the jet mass must satisfy $55 < m_J < 65$ GeV. The CRs for validation tests are redefined by removing the events in the vSR. The vSR and analogous CRs are used to compute the analog of α, and the full background prediction is evaluated on data. The predicted yields in the vSR are then compared to the observed event yields. This comparison is performed in the corresponding vSR of each of the event categories. The resulting distributions are shown in Fig. 5.

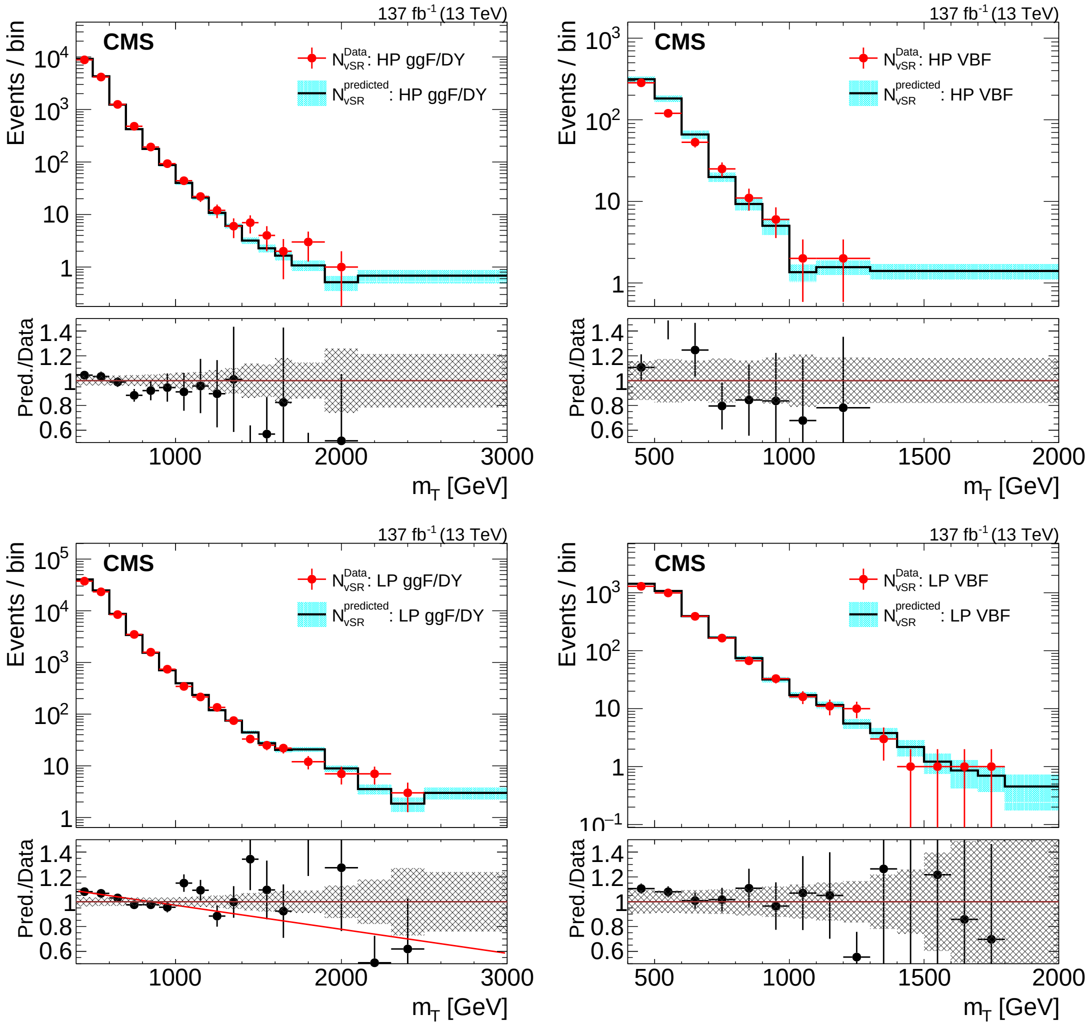

Figure 5: Comparison of background estimations and observations in the high-purity ggF/DY (upper left), high-purity VBF (upper right), low-purity ggF/DY (lower left), and low-purity VBF (lower right) validation signal regions. The lower panel shows the ratio of the estimated and the observed event yields. The hashed band in the ratio represents the total uncertainty in the corresponding SR. The red line (lower left) is a fit to the ratio of prediction to the data in the LP ggF/DY vSR.

The vSR tests result in a prediction of more events in each of the event categories than observed in the data. The overprediction is as large as 10% in the lowest m_T bin. To account for any potential mismodeling of our prediction, we derive a shape uncertainty. The uncertainty is based on a linear fit to the ratio of the prediction and the observation versus m_T in the LP ggF/DY vSR. Based on the fit, an uncertainty is assessed that corresponds to 7% in the lowest m_T bin, and decreases linearly to -40% in the highest m_T bin. This shape uncertainty is applied to each of the four signal regions assuming no correlation between the regions.

7 Systematic uncertainties

Because the nonresonant backgrounds are estimated from data, several simulation-related systematic uncertainties have little to no effect on the estimation of these backgrounds. However, PDF uncertainties, renormalization (μ_R) and factorization (μ_F) scale uncertainties, and jet energy scale (JES) and resolution (JER) uncertainties have nonnegligible effects on α.

For PDF uncertainties, the distribution of α is evaluated for each recommended PDF variation [31, 32]. An envelope of these variations is used to assess an α shape uncertainty. The size of the uncertainty in a given m_T bin due to PDFs is as large as 3 (1.5)% for the VBF (ggF/DY) categories. The effects of the scale uncertainties are evaluated by varying the values of μ_R and μ_F simultaneously up and down by a factor of two. Based on scale variations, an α shape uncertainty is determined, which is less than 2% in any single m_T bin. The JES and JER uncertainties are propagated to α, and are not larger than 3%. A summary of all systematic uncertainties related to the nonresonant background prediction is shown in the second and third columns of Table 2.

In addition to those listed in Table 2, we account for uncertainties due to the limited size of simulated data sets. The Poisson uncertainties associated with the observed CR yields are propagated to the nonresonant background predictions in each m_T bin. The uncertainties due to the limited size of simulated data sets are treated as uncorrelated across each analysis bin.

The predicted resonant background and signal yield uncertainties are evaluated from a larger list of potential sources. These sources include the integrated luminosity, τ_{21} scale factors, pileup modeling, b jet veto efficiency, effects related to inefficiencies due to instrumental effects of the electromagnetic calorimeter trigger (prefiring), modeling of unclustered energy in the calculation of p_T^{miss}, jet mass scale (JMS) and resolution (JMR), JES and JER, trigger efficiency modeling, PDF uncertainties, and scale uncertainties. A summary of the impacts these uncertainties have on resonant backgrounds and signal is shown in the fourth through seventh columns of Table 2 and in Table 3. A description of each uncertainty source is provided below.

The measured integrated luminosity uncertainty is propagated to the prediction of the resonant background and signal yields. This uncertainty amounts to 1.6% on the entire data set [64–66] and is correlated across all signal regions. The effects of the luminosity uncertainty on signal and nonresonant backgrounds are treated as fully correlated.

Uncertainties associated with the determination of τ_{21} efficiency scale factors that correct for systematic differences in simulated and collision data sets are propagated to the predicted signal and resonant background yields. These uncertainties have two components: one that affects the normalization of predictions (τ_{21} SF) and another that accounts for p_T-dependent differences (τ_{21} p_T extrap.) in the tagging efficiency, which affects the m_T shape of our predicted yields.

Jet energy and jet mass scales are varied within their uncertainties. Effects of JMS uncertainties are treated as anticorrelated between SR and CR regions and correlated across all categories. The magnitudes of JMS uncertainties are assumed to be independent of m_T. They are treated as fully correlated across all m_T bins and all regions.

Jet masses are smeared to broaden their distribution within measured JMR uncertainties. Jet mass smearing is done for both SR and CR but for simulated data sets only. The effect of jet smearing was at most 10%. The effects of JMR uncertainties are correlated across m_T bins and all categories, and between signals and resonant backgrounds.

Similarly to the nonresonant background, the effect of JES and JER uncertainties are propagated to the predicted event yields. These are found to have minimal impact on the m_T shape (<1%) within a given category but can cause events to migrate from the ggF/DY to the VBF categories.

Other systematic uncertainties affect the normalization of resonant backgrounds and signals. These include pileup uncertainties, b-tagging scale factor uncertainties, prefiring corrections, unclustered energy scale uncertainties, and trigger uncertainties. These effects are assumed to be correlated across various categories, and between signal and resonant backgrounds.

Finally, the statistical uncertainties due to the limited size of simulated data sets are propagated to all predicted signal and resonant background yields. In this analysis, all the uncertainties quoted are pre-fit values.

Table 2: Summary of systematic uncertainties (in %) related to the SM background predictions in various regions. Columns two and three tabulate the representative size of effects on α in the VBF and ggF/DY events categories, respectively. Columns four through seven tabulate the typical size of effects on the prediction of resonant background yields in the VBF SR, VBF CR, ggF/DY SR, and ggF/DY CR, respectively. All of these numbers are the pre-fit values. For some systematic uncertainties, the variation in different m_T bins are shown as a range. Values of LP that are different from those of HP are shown in parentheses.

Source	α_{VBF}	$\alpha_{ggF/DY}$	VBF SR	VBF CR	ggF/DY SR	ggF/DY CR
Luminosity	—	—	1.6	1.6	1.6	1.6
τ_{21} SF	—	—	7.3 (17.0)	7.3 (17.0)	7.3 (17.0)	7.3 (17.0)
τ_{21} p_T extrap.	—	—	2–18 (1–10)	2–18 (1–10)	2–18 (1–10)	2–18 (1–10)
Pileup	—	—	3.9 (3.9)	2.0 (3.7)	1.0 (0.8)	1.7 (0.9)
b jet veto	—	—	2.4 (2.9)	3.5 (3.2)	1.8 (2.2)	2.8 (2.6)
Prefiring	—	—	0.7 (0.6)	0.8 (0.7)	0.3 (0.2)	0.4 (0.3)
Unclustered energy	—	—	2.4 (1.6)	1.8 (1.4)	1.8 (1.3)	1.6 (1.5)
JMS	—	—	0.5 (0.4)	1.8 (0.5)	0.3 (0.3)	1.6 (0.4)
JMR	—	—	1.2 (1.6)	5.9 (0.7)	1.7 (1.01)	7.1 (0.96)
Trigger	—	—	1.4	1.4	1.4	1.4
JES	3.0	1–2	40–13	40–13	4.0	4.0
JER	3.0	1.5	35–13	35–13	2.0	2.0
PDF norm.	—	—	5.0	5.0	2.0	2.0
PDF shape	3.0	1.5	0.5–4	0.5–4	0.5–4	0.5–4
μ_R, μ_F norm.	—	—	15	15	11	12
μ_R, μ_F shape	1–2	1–2	1–10	2–4	3–8	3–4
Nonclosure	7–40	7–40	—	—	—	—

8 Results and interpretations

The final predicted event yields are computed using a simultaneous maximum likelihood fit of event yields in all m_T bins, and all SRs and CRs. Each bin is modeled as a marked Poisson model [67] with mean value corresponding to the sum of expected yields for resonant and

Table 3: Summary of the typical size of systematic uncertainties (in %) in the predicted signal yields in various regions. All of these numbers are the pre-fit values. A range is given for the shape systematic uncertainties. Values of LP that are different from those of HP are shown in parentheses.

Source	VBF SR	VBF CR	ggF/DY SR	ggF/DY CR
Luminosity	1.6	1.6	1.6	1.6
τ_{21} SF	7.3 (17.0)	7.3 (17.0)	7.3 (17.0)	7.3 (17.0)
τ_{21} p_{T} extrap.	2–18 (1–10)	2–18 (1–10)	2–18 (1–10)	2–18 (1–10)
Pileup	0.2 (0.5)	0.7 (1.0)	1.1 (0.9)	1.1 (0.6)
b jet veto	1.3 (1.4)	1.4 (1.6)	1.3 (1.4)	1.3 (1.5)
Prefiring	1.0 (0.9)	1.0 (1.0)	0.6 (0.5)	0.6 (0.5)
Unclustered energy	0.1	0.1	0.1	0.1
JMS	0.9 (0.3)	2.6 (1.9)	0.7 (0.3)	2.4 (1.5)
JMR	3.2 (2.8)	6.9 (4.0)	3.3 (2.4)	7.5 (3.4)
Trigger	1.4 (1.4)	1.4 (1.5)	1.4 (1.6)	1.4 (1.5)
JES	5–11	4–14	1–7	1–5
JER	2–3	6–7	1–7	1–5

nonresonant backgrounds, and signal. An unconstrained nuisance parameter is implemented to allow for the fit to independently adjust the nonresonant background in each m_{T} bin of each category. For each m_{T} bin of each event category, this constraint is fully correlated between the SR and CR. Systematic uncertainties are implemented using log-normal priors. The likelihood is parameterized in terms of the signal strength μ, which is the ratio of the measured signal cross section and the theoretical cross section.

The predicted event yields for all backgrounds and a graviton ($m_{\mathrm{G}} = 1\,\mathrm{TeV}$) are shown in Fig. 6 (7) for the CR (SR). The data are compared to post-fit predictions, where fit refers to constraints on predictions and their uncertainties based on a maximum likelihood fit to data in which the signal strength is fixed to $\mu = 0$. The post-fit predictions and observations are consistent within the uncertainties, suggesting no evidence of new sources of diboson production.

We derive both expected and observed 95% confidence level (CL) upper limits on the $\mathrm{X} \to \mathrm{V}(\mathrm{q\overline{q}})\mathrm{Z}(\nu\overline{\nu})$ production cross section. A test statistic is used in conjunction with the $\mathrm{CL_s}$ criterion [68] to set upper limits. The test statistic is defined as $q_\mu = -2\ln(\mathcal{L}_\mu/\mathcal{L}_{\mathrm{max}})$, where $\mathcal{L}_{\mathrm{max}}$ refers to the maximum value of the likelihood when all parameters are varied and $\mathcal{L}_\mu$ refers to the likelihood obtained by varying μ while profiling all the other parameters conditioned on its value. Upper limits are computed using the asymptotic approximation [69]. Expected limits are computed by evaluating the test statistic using the post-fit predicted numbers of background events and their uncertainties.

Upper limits on the radion production cross sections times their branching fraction to ZZ versus the radion mass are shown in Fig. 8. Limits are computed assuming radions are produced entirely either through the ggF process or the VBF process. The expected (observed) radion mass exclusion limits are 2.5 (3.0) TeV for ggF-produced states. These are the first mass exclusion limits set by CMS on ggF-produced radions in this final state. Figure 9 shows the expected and observed upper limits on the W′ boson production cross sections times their branching fraction to WZ, assuming exclusive production through the DY (model B) or VBF process (model C). The expected and observed mass exclusion limits for DY-produced W′ resonances are found to be 3.7 and 4.0 TeV, respectively. This is an improvement of 0.6 (0.4) TeV in the observed (expected) mass exclusion limit from the previous CMS result. Finally, the upper limits on the graviton production cross sections times their branching fraction to ZZ are shown

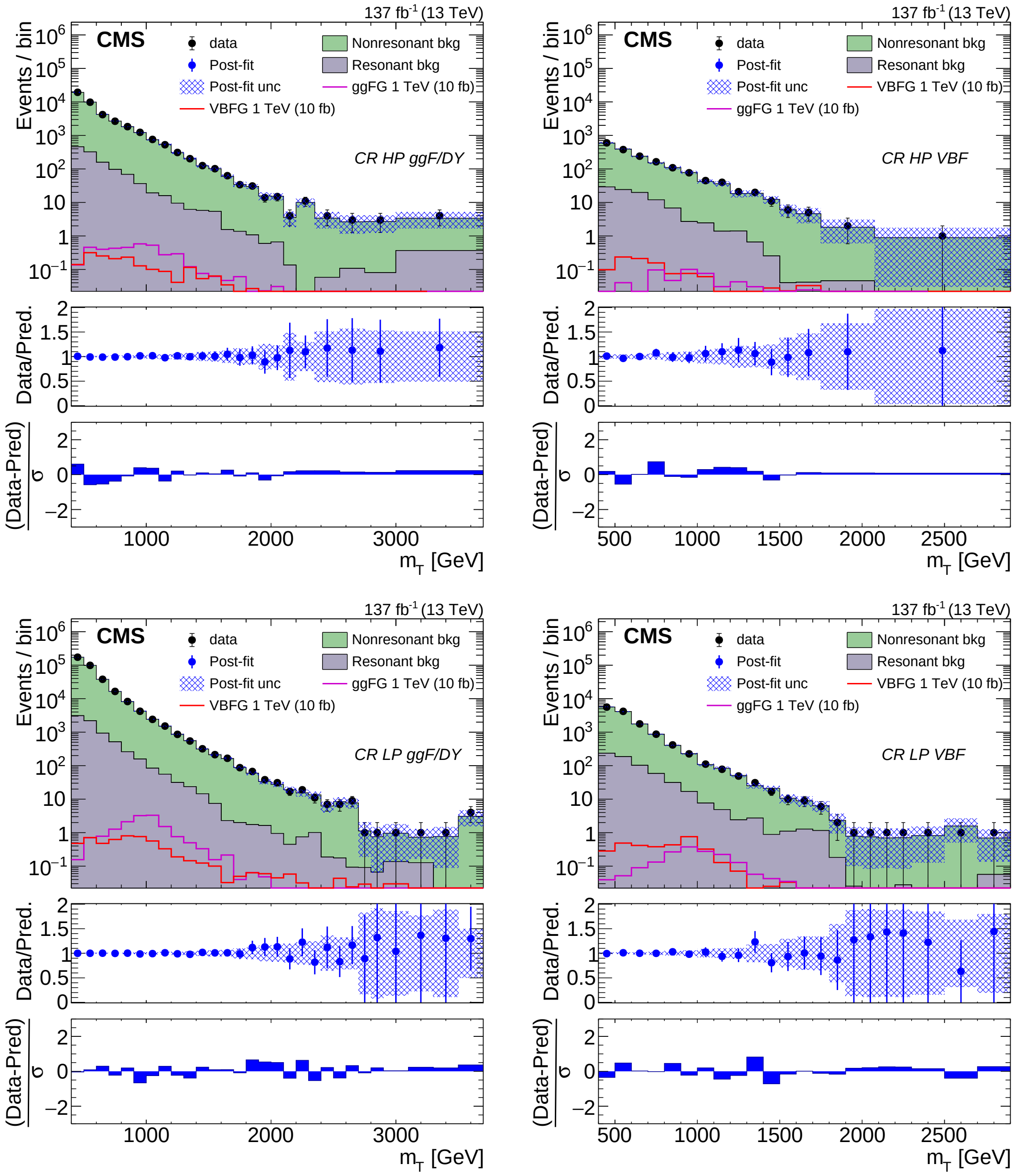

Figure 6: Distributions of m_T for high-purity ggF/DY (upper left) and VBF (upper right), and low-purity ggF/DY (lower left) and VBF (lower right) CR events after performing background-only fits. The last bin in the upper left, upper right, lower left, and lower right plot corresponds to the yields integrated above 3, 2.3, 3.5, and 2.7 TeV, respectively. The top panel of each plot shows the post-fit prediction, represented by filled histograms, compared to observed yields, represented by black points. Both the ggF and VBF-produced 1 TeV graviton signals are shown in each plot, represented by the open purple and red histograms, respectively. The signal is normalized to 10 fb. The blue hashed area represents the total uncertainty from the post-fit predicted event yield as a function of m_T. The middle panel of each plot shows the ratio of data and post-fit predictions in blue. The bottom panel of each plot shows the difference between the observed event yields and the post-fit predictions normalized by the quadratic sum of the statistical uncertainty of the observed yield and the total uncertainty from the post-fit prediction in each m_T bin.

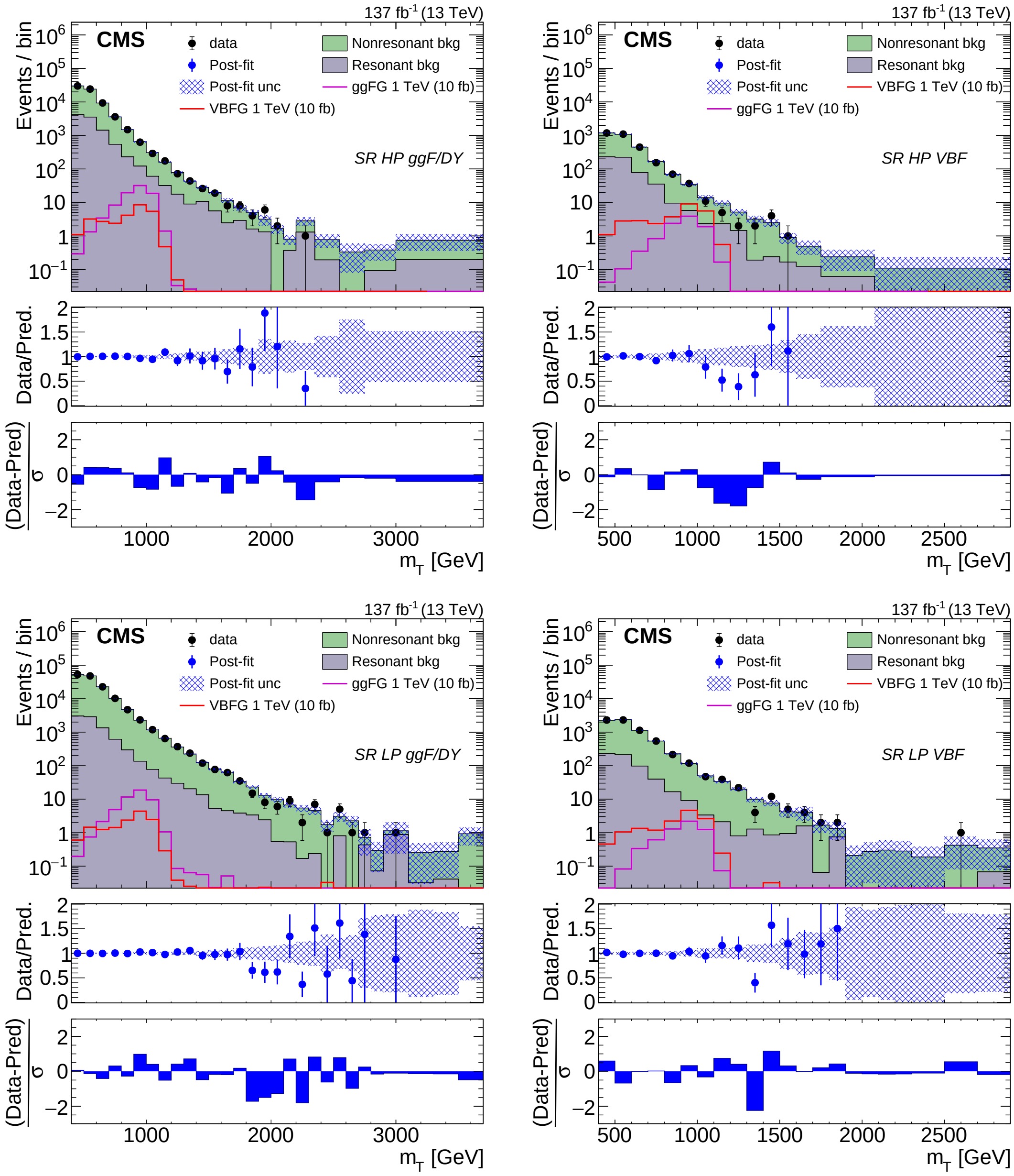

Figure 7: Distribution of the predicted and observed event yields versus m_T for high-purity ggF/DY (upper left) and VBF (upper right), and low-purity ggF/DY (lower left) and VBF (lower right) SR events. The last bin in each plot corresponds to the yields integrated above the penultimate bin. The top panel of each plot shows the prediction based on a background-only fit to data, represented by filled histograms, compared to observed yields, represented by black points. Both the ggF and VBF-produced 1 TeV graviton signals are shown in each plot, represented by the open purple and red histograms, respectively. The signal is normalized to 10 fb. The middle panel of each plot shows the ratio of data and post-fit predictions in blue. The blue hashed area represents the total uncertainty from the post-fit predicted event yield as a function of m_T. The bottom panel of each plot shows the difference between the observed event yields and the post-fit predictions normalized by the quadratic sum of the statistical uncertainty of the observed yield and the total uncertainty from the post-fit prediction in each m_T bin.

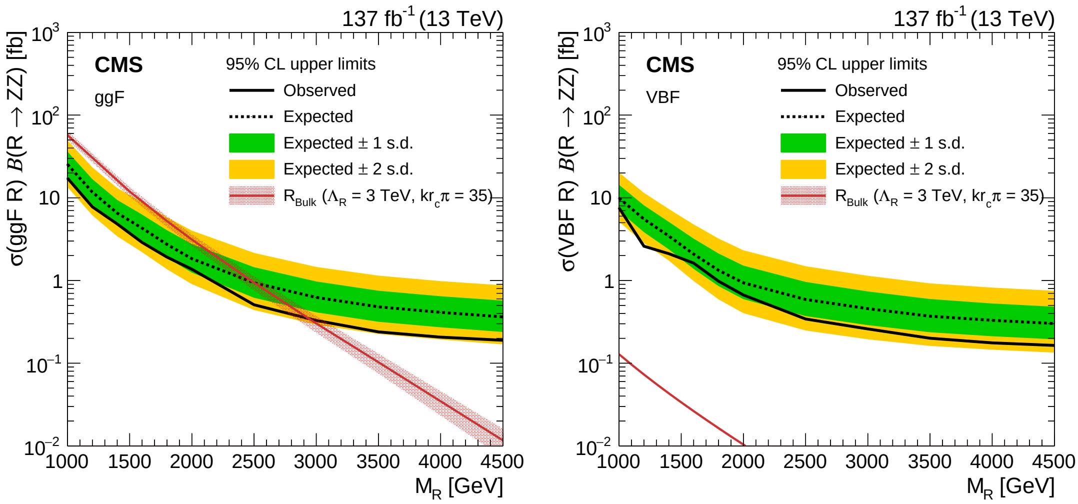

Figure 8: Expected and observed 95% CL upper limits on the radion (R) production cross section times the R $\to$ ZZ branching fraction versus the radion mass are shown as dashed and solid black lines, respectively. Green and yellow bands, respectively, represent the 68% and 95% confidence intervals of the expected limit. The red curves show the theoretical radion production cross sections times their branching fractions to ZZ. The hashed red areas represent the theoretical cross section uncertainty due to limited knowledge of PDFs and scale choices. Limits and theory cross sections for ggF-produced radions are shown in the left figure, while the right figure shows the same for VBF-produced radions.

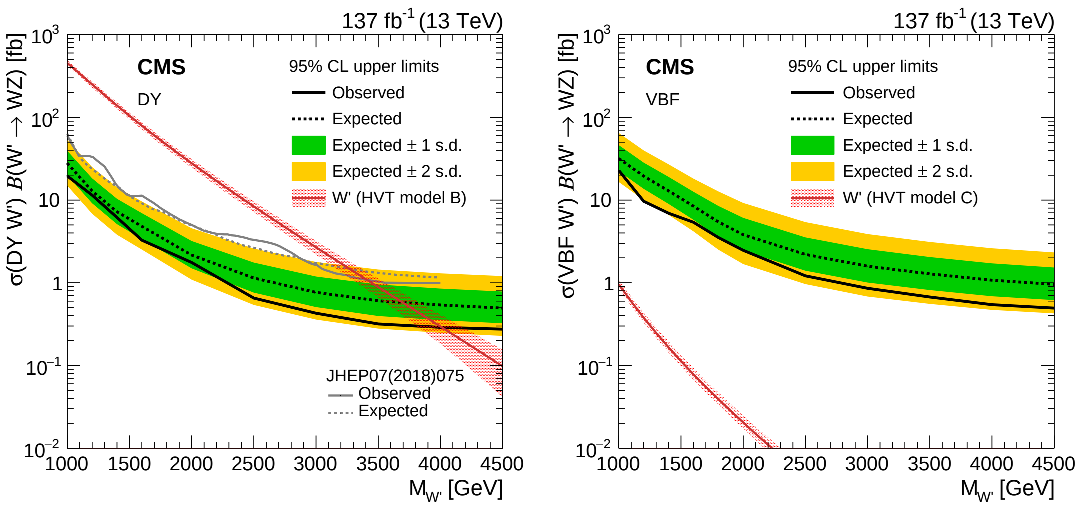

Figure 9: Expected and observed 95% CL upper limits on the W′ production cross section times the W′ $\to$ WZ branching fraction versus the W′ mass are shown as dashed and solid black lines, respectively. Green and yellow bands, respectively, represent the 68% and 95% confidence intervals of the expected limit. The red curves show the theoretical W′ boson production cross sections times their branching fractions to WZ. The hashed red areas represent the theoretical cross section uncertainty due to limited knowledge of PDFs and scale choices. Limits and theory cross sections for DY-produced W′ bosons are shown in the left figure, while the right figure shows the same for VBF-produced W′ bosons. The grey curves in the left plot show the previous CMS results with 36 fb^{-1} of data.

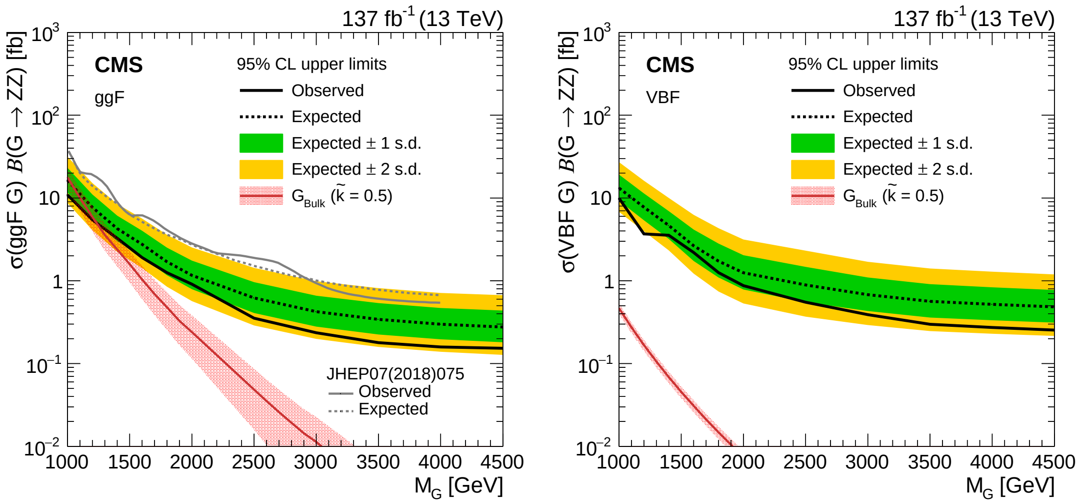

Figure 10: Expected and observed 95% CL upper limits on the graviton (G) production cross section times the $G \to ZZ$ branching fraction versus the graviton mass are shown as dashed and solid black lines, respectively. Green and yellow bands, respectively, represent 68% and 95% confidence intervals of the expected limit. The red curves show the theoretical graviton production cross sections times their branching fractions to ZZ. The hashed red areas represent the theoretical cross section uncertainty due to limited knowledge of PDFs and scale choices. Limits and theory cross sections for ggF-produced gravitons are shown in the left figure, while the right figure shows the same for VBF-produced gravitons. The grey curves in the left plot show the previous CMS results with 36 fb^{-1} of data.

in Fig. 10. Limits are set assuming gravitons are produced entirely either through the ggF process or the VBF process. The expected (observed) graviton mass exclusion limit is found to be 1.1 (1.2) TeV, assuming gravitons are produced exclusively through the ggF mechanism. These are the first mass exclusion limits set by CMS on ggF-produced gravitons in this final state. For the VBF-produced models considered here, no masses are excluded. The observed upper limits on $\sigma\mathcal{B}(X \to VZ)$ vary between 0.2 and 9 fb for radions, 0.5 and 20 fb for W$'$ resonances, and 0.3 and 10 fb for gravitons.

The methods used here complement the recent ATLAS search [14] in the same channel by using different jet substructure variables and different VBF tagging requirements. The 95% CL upper limits on these resonance production cross sections times $X \to Z + W/Z$ branching fraction from the recent ATLAS results are comparable to those set in this paper.

9 Summary

A search has been presented for new bosonic states decaying either to a pair of Z bosons or to a W boson and a Z boson. The analyzed final states require large missing transverse momentum and one high-momentum, large-radius jet. Large-radius jets are required to have a mass consistent with either a W or Z boson. Events are categorized based on the presence of large-radius jets passing high-purity and low-purity substructure requirements. Events are also categorized based on the presence or absence of high-momentum jets in the forward region of the detector. Forward jets distinguish weak vector boson fusion (VBF) from other production mechanisms. Contributions from the dominant SM backgrounds are estimated from data control regions using an extrapolation method. No deviation between SM expectation and data is found, and 95% confidence level upper limits are set on the production cross section times branching fraction for several signal models. A lower observed (expected) limit of 3.0 (2.5) TeV is set on the mass of gluon-gluon fusion produced radions. The observed (expected) mass exclusion limit for Drell–Yan produced W' bosons is found to be 4.0 (3.7) TeV. The observed (expected) mass exclusion limit for gluon-gluon fusion produced gravitons is found to be 1.2 (1.1) TeV. At 95% confidence level, upper observed (expected) limits on the VBF production cross section times $X \rightarrow Z + W/Z$ branching fraction range between 0.2 and 20 (0.3 and 30) fb. The 95% CL upper limits on these resonance production cross sections times $X \rightarrow Z + W/Z$ branching fraction from the recent ATLAS results are comparable to those set in this paper.

Acknowledgments

We congratulate our colleagues in the CERN accelerator departments for the excellent performance of the LHC and thank the technical and administrative staffs at CERN and at other CMS institutes for their contributions to the success of the CMS effort. In addition, we gratefully acknowledge the computing centers and personnel of the Worldwide LHC Computing Grid and other centers for delivering so effectively the computing infrastructure essential to our analyses. Finally, we acknowledge the enduring support for the construction and operation of the LHC, the CMS detector, and the supporting computing infrastructure provided by the following funding agencies: BMBWF and FWF (Austria); FNRS and FWO (Belgium); CNPq, CAPES, FAPERJ, FAPERGS, and FAPESP (Brazil); MES and BNSF (Bulgaria); CERN; CAS, MoST, and NSFC (China); MINCIENCIAS (Colombia); MSES and CSF (Croatia); RIF (Cyprus); SENESCYT (Ecuador); MoER, ERC PUT and ERDF (Estonia); Academy of Finland, MEC, and HIP (Finland); CEA and CNRS/IN2P3 (France); BMBF, DFG, and HGF (Germany); GSRI (Greece); NKFIA (Hungary); DAE and DST (India); IPM (Iran); SFI (Ireland); INFN (Italy); MSIP and NRF (Republic of Korea); MES (Latvia); LAS (Lithuania); MOE and UM (Malaysia); BUAP, CINVESTAV, CONACYT, LNS, SEP, and UASLP-FAI (Mexico); MOS (Montenegro); MBIE (New Zealand); PAEC (Pakistan); MSHE and NSC (Poland); FCT (Portugal); JINR (Dubna); MON, RosAtom, RAS, RFBR, and NRC KI (Russia); MESTD (Serbia); SEIDI, CPAN, PCTI, and FEDER (Spain); MOSTR (Sri Lanka); Swiss Funding Agencies (Switzerland); MST (Taipei); ThEPCenter, IPST, STAR, and NSTDA (Thailand); TUBITAK and TAEK (Turkey); NASU (Ukraine); STFC (United Kingdom); DOE and NSF (USA).

Individuals have received support from the Marie-Curie program and the European Research Council and Horizon 2020 Grant, contract Nos. 675440, 724704, 752730, 758316, 765710, 824093, 884104, and COST Action CA16108 (European Union); the Leventis Foundation; the Alfred P. Sloan Foundation; the Alexander von Humboldt Foundation; the Belgian Federal Science Policy Office; the Fonds pour la Formation à la Recherche dans l'Industrie et dans l'Agriculture (FRIA-Belgium); the Agentschap voor Innovatie door Wetenschap en Technologie (IWT-Belgium); the F.R.S.-FNRS and FWO (Belgium) under the "Excellence of Science – EOS" – be.h project n. 30820817; the Beijing Municipal Science & Technology Commission, No. Z191100007219010; the Ministry of Education, Youth and Sports (MEYS) of the Czech Republic; the Deutsche Forschungsgemeinschaft (DFG), under Germany's Excellence Strategy – EXC 2121 "Quantum Universe" – 390833306, and under project number 400140256 - GRK2497; the Lendület ("Momentum") Program and the János Bolyai Research Scholarship of the Hungarian Academy of Sciences, the New National Excellence Program ÚNKP, the NKFIA research grants 123842, 123959, 124845, 124850, 125105, 128713, 128786, and 129058 (Hungary); the Council of Science and Industrial Research, India; the Latvian Council of Science; the Ministry of Science and Higher Education and the National Science Center, contracts Opus 2014/15/B/ST2/03998 and 2015/19/B/ST2/02861 (Poland); the Fundação para a Ciência e a Tecnologia, grant CEECIND/01334/2018 (Portugal); the National Priorities Research Program by Qatar National Research Fund; the Ministry of Science and Higher Education, project no. 14.W03.31.0026 (Russia); the Programa Estatal de Fomento de la Investigación Científica y Técnica de Excelencia María de Maeztu, grant MDM-2015-0509 and the Programa Severo Ochoa del Principado de Asturias; the Stavros Niarchos Foundation (Greece); the Rachadapisek Sompot Fund for Postdoctoral Fellowship, Chulalongkorn University and the Chulalongkorn Academic into Its 2nd Century Project Advancement Project (Thailand); the Kavli Foundation; the Nvidia Corporation; the SuperMicro Corporation; the Welch Foundation, contract C-1845; and the Weston Havens Foundation (USA).

References

[1] L. Randall and R. Sundrum, "Large mass hierarchy from a small extra dimension", *Phys. Rev. Lett.* **83** (1999) 3370, doi:10.1103/physrevlett.83.3370, arXiv:hep-ph/9905221.

[2] L. Randall and R. Sundrum, "An alternative to compactification", *Phys. Rev. Lett.* **83** (1999) 4690, doi:10.1103/physrevlett.83.4690, arXiv:hep-th/9906064.

[3] K. Agashe et al., "LHC signals for warped electroweak charged gauge bosons", *Phys. Rev. D* **80** (2009) 075007, doi:10.1103/PhysRevD.80.075007, arXiv:0810.1497.

[4] K. Agashe et al., "LHC signals for coset electroweak gauge bosons in warped/composite pseudo-Goldstone boson Higgs models", *Phys. Rev. D* **81** (2010) 096002, doi:10.1103/PhysRevD.81.096002, arXiv:0911.0059.

[5] K. Agashe et al., "CERN LHC signals for warped electroweak neutral gauge bosons", *Phys. Rev. D* **76** (2007) 115015, doi:10.1103/PhysRevD.76.115015, arXiv:0709.0007.

[6] D. Pappadopulo, A. Thamm, R. Torre, and A. Wulzer, "Heavy vector triplets: Bridging theory and data", *JHEP* **09** (2014) 060, doi:10.1007/JHEP09(2014)060, arXiv:1402.4431.

[7] N. Arkani-Hamed et al., "The minimal moose for a little Higgs", *JHEP* **08** (2002) 021, doi:10.1088/1126-6708/2002/08/021, arXiv:hep-ph/0206020.

[8] N. Arkani-Hamed, A. G. Cohen, E. Katz, and A. E. Nelson, "The littlest Higgs", *JHEP* **07** (2002) 034, doi:10.1088/1126-6708/2002/07/034, arXiv:hep-ph/0206021.

[9] G. Burdman, M. Perelstein, and A. Pierce, "Large Hadron Collider tests of the little Higgs model", *Phys. Rev. Lett.* **90** (2003) 241802, doi:10.1103/PhysRevLett.90.241802, arXiv:hep-ph/0212228. [Erratum: doi:10.1103/PhysRevLett.92.049903].

[10] K. Agashe, H. Davoudiasl, G. Perez, and A. Soni, "Warped gravitons at the CERN LHC and beyond", *Phys. Rev. D* **76** (2007) 036006, doi:10.1103/PhysRevD.76.036006, arXiv:hep-ph/0701186.

[11] A. L. Fitzpatrick, J. Kaplan, L. Randall, and L.-T. Wang, "Searching for the Kaluza-Klein graviton in bulk RS models", *JHEP* **09** (2007) 013, doi:10.1088/1126-6708/2007/09/013, arXiv:hep-ph/0701150.

[12] ATLAS Collaboration, "Searches for heavy ZZ and ZW resonances in the $\ell\ell qq$ and $\nu\nu qq$ final states in pp collisions at $\sqrt{s} = 13$ TeV with the ATLAS detector", *JHEP* **03** (2018) 009, doi:10.1007/JHEP03(2018)009, arXiv:1708.09638.

[13] CMS Collaboration, "Search for a heavy resonance decaying into a Z boson and a vector boson in the $\nu\overline{\nu}\mathrm{q}\overline{\mathrm{q}}$ final state", *JHEP* **07** (2018) 075, doi:10.1007/JHEP07(2018)075, arXiv:1803.03838.

[14] ATLAS Collaboration, "Search for heavy diboson resonances in semileptonic final states in pp collisions at $\sqrt{s} = 13$ TeV with the ATLAS detector", *Eur. Phys. J. C* **80** (2020) 1165, doi:10.1140/epjc/s10052-020-08554-y, arXiv:2004.14636.

[15] "HEPData record for this analysis", 2021. doi:10.17182/hepdata.103856.

[16] CMS Collaboration, "Performance of the CMS Level-1 trigger in proton-proton collisions at $\sqrt{s} = 13\,\mathrm{TeV}$", *JINST* **15** (2020) P10017, doi:10.1088/1748-0221/15/10/P10017, arXiv:2006.10165.

[17] CMS Collaboration, "The CMS trigger system", *JINST* **12** (2017) P01020, doi:10.1088/1748-0221/12/01/P01020, arXiv:1609.02366.

[18] CMS Collaboration, "The CMS experiment at the CERN LHC", *JINST* **3** (2008) S08004, doi:10.1088/1748-0221/3/08/S08004.

[19] J. Alwall et al., "The automated computation of tree-level and next-to-leading order differential cross sections, and their matching to parton shower simulations", *JHEP* **07** (2014) 079, doi:10.1007/JHEP07(2014)079, arXiv:1405.0301.

[20] R. Frederix and S. Frixione, "Merging meets matching in MC@NLO", *JHEP* **12** (2012) 061, doi:10.1007/JHEP12(2012)061, arXiv:1209.6215.

[21] J. Alwall et al., "Comparative study of various algorithms for the merging of parton showers and matrix elements in hadronic collisions", *Eur. Phys. J. C* **53** (2008) 473, doi:10.1140/epjc/s10052-007-0490-5, arXiv:0706.2569.

[22] P. Artoisenet, R. Frederix, O. Mattelaer, and R. Rietkerk, "Automatic spin-entangled decays of heavy resonances in Monte Carlo simulations", *JHEP* **03** (2013) 015, doi:10.1007/JHEP03(2013)015, arXiv:1212.3460.

[23] P. Nason, "A new method for combining NLO QCD with shower Monte Carlo algorithms", *JHEP* **11** (2004) 040, doi:10.1088/1126-6708/2004/11/040, arXiv:hep-ph/0409146.

[24] S. Frixione, P. Nason, and C. Oleari, "Matching NLO QCD computations with parton shower simulations: the POWHEG method", *JHEP* **11** (2007) 070, doi:10.1088/1126-6708/2007/11/070, arXiv:0709.2092.

[25] S. Alioli, P. Nason, C. Oleari, and E. Re, "A general framework for implementing NLO calculations in shower Monte Carlo programs: the POWHEG BOX", *JHEP* **06** (2010) 043, doi:10.1007/JHEP06(2010)043, arXiv:1002.2581.

[26] S. Alioli, P. Nason, C. Oleari, and E. Re, "NLO single-top production matched with shower in POWHEG: *s*- and *t*-channel contributions", *JHEP* **09** (2009) 111, doi:10.1088/1126-6708/2009/09/111, arXiv:0907.4076. [Erratum: doi:10.1007/JHEP02(2010)011].

[27] E. Re, "Single-top Wt-channel production matched with parton showers using the POWHEG method", *Eur. Phys. J. C* **71** (2011) 1547, doi:10.1140/epjc/s10052-011-1547-z, arXiv:1009.2450.

[28] T. Sjöstrand et al., "An introduction to PYTHIA 8.2", *Comput. Phys. Commun.* **191** (2015) 159, doi:10.1016/j.cpc.2015.01.024, arXiv:1410.3012.

[29] CMS Collaboration, "Event generator tunes obtained from underlying event and multiparton scattering measurements", *Eur. Phys. J. C* **76** (2016) 155, doi:10.1140/epjc/s10052-016-3988-x, arXiv:1512.00815.

[30] CMS Collaboration, "Extraction and validation of a new set of CMS PYTHIA8 tunes from underlying-event measurements", *Eur. Phys. J. C* **80** (2020) 4, doi:10.1140/epjc/s10052-019-7499-4, arXiv:1903.12179.

[31] NNPDF Collaboration, "Parton distributions for the LHC Run II", *JHEP* **04** (2015) 040, doi:10.1007/JHEP04(2015)040, arXiv:1410.8849.

[32] NNPDF Collaboration, "Parton distributions from high-precision collider data", *Eur. Phys. J. C* **77** (2017) 663, doi:10.1140/epjc/s10052-017-5199-5, arXiv:1706.00428.

[33] GEANT4 Collaboration, "GEANT4—a simulation toolkit", *Nucl. Instrum. Meth. A* **506** (2003) 250, doi:10.1016/S0168-9002(03)01368-8.

[34] T. Melia, P. Nason, R. Rontsch, and G. Zanderighi, "W^+W^-, WZ and ZZ production in the POWHEG BOX", *JHEP* **11** (2011) 078, doi:10.1007/JHEP11(2011)078, arXiv:1107.5051.

[35] M. Beneke, P. Falgari, S. Klein, and C. Schwinn, "Hadronic top-quark pair production with NNLL threshold resummation", *Nucl. Phys. B* **855** (2012) 695, doi:10.1016/j.nuclphysb.2011.10.021, arXiv:1109.1536.

[36] M. Cacciari et al., "Top-pair production at hadron colliders with next-to-next-to-leading logarithmic soft-gluon resummation", *Phys. Lett. B* **710** (2012) 612, doi:10.1016/j.physletb.2012.03.013, arXiv:1111.5869.

[37] P. Bärnreuther, M. Czakon, and A. Mitov, "Percent-level-precision physics at the Tevatron: Next-to-next-to-leading order QCD corrections to $q\overline{q} \to t\overline{t} + X$", *Phys. Rev. Lett.* **109** (2012) 132001, doi:10.1103/PhysRevLett.109.132001, arXiv:1204.5201.

[38] M. Czakon and A. Mitov, "NNLO corrections to top-pair production at hadron colliders: the all-fermionic scattering channels", *JHEP* **12** (2012) 054, doi:10.1007/JHEP12(2012)054, arXiv:1207.0236.

[39] M. Czakon and A. Mitov, "NNLO corrections to top pair production at hadron colliders: the quark-gluon reaction", *JHEP* **01** (2013) 080, doi:10.1007/JHEP01(2013)080, arXiv:1210.6832.

[40] M. Czakon, P. Fiedler, and A. Mitov, "Total top-quark pair-production cross section at hadron colliders through $O(\alpha_S^4)$", *Phys. Rev. Lett.* **110** (2013) 252004, doi:10.1103/PhysRevLett.110.252004, arXiv:1303.6254.

[41] R. Gavin, Y. Li, F. Petriello, and S. Quackenbush, "W physics at the LHC with FEWZ 2.1", *Comput. Phys. Commun.* **184** (2013) 208, doi:10.1016/j.cpc.2012.09.005, arXiv:1201.5896.

[42] R. Gavin, Y. Li, F. Petriello, and S. Quackenbush, "FEWZ 2.0: A code for hadronic Z production at next-to-next-to-leading order", *Comput. Phys. Commun.* **182** (2011) 2388, doi:10.1016/j.cpc.2011.06.008, arXiv:1011.3540.

[43] J. M. Lindert et al., "Precise predictions for V+jets dark matter backgrounds", *Eur. Phys. J. C* **77** (2017) 829, doi:10.1140/epjc/s10052-017-5389-1, arXiv:1705.04664.

[44] S. Bolognesi et al., "Spin and parity of a single-produced resonance at the LHC", *Phys. Rev. D* **86** (2012) 095031, doi:10.1103/PhysRevD.86.095031, arXiv:1208.4018.

[45] A. Oliveira, "Gravity particles from warped extra dimensions, predictions for LHC", 2014. arXiv:1404.0102.

[46] CMS Collaboration, "Particle-flow reconstruction and global event description with the CMS detector", *JINST* **12** (2017) P10003, doi:10.1088/1748-0221/12/10/P10003, arXiv:1706.04965.

[47] M. Cacciari, G. P. Salam, and G. Soyez, "The anti-k_T jet clustering algorithm", *JHEP* **04** (2008) 063, doi:10.1088/1126-6708/2008/04/063, arXiv:0802.1189.

[48] M. Cacciari, G. P. Salam, and G. Soyez, "FastJet user manual", *Eur. Phys. J. C* **72** (2012) 1896, doi:10.1140/epjc/s10052-012-1896-2, arXiv:1111.6097.

[49] CMS Collaboration, "Performance of electron reconstruction and selection with the CMS detector in proton-proton collisions at $\sqrt{s} = 8$ TeV", *JINST* **10** (2015) P06005, doi:10.1088/1748-0221/10/06/P06005, arXiv:1502.02701.

[50] CMS Collaboration, "Performance of the CMS muon detector and muon reconstruction with proton-proton collisions at $\sqrt{s} = 13$ TeV", *JINST* **13** (2018) P06015, doi:10.1088/1748-0221/13/06/P06015, arXiv:1804.04528.

[51] K. Rehermann and B. Tweedie, "Efficient identification of boosted semileptonic top quarks at the LHC", *JHEP* **03** (2011) 059, doi:10.1007/JHEP03(2011)059, arXiv:1007.2221.

[52] CMS Collaboration, "Performance of photon reconstruction and identification with the CMS detector in proton-proton collisions at $\sqrt{s} = 8$ TeV", *JINST* **10** (2015) P08010, doi:10.1088/1748-0221/10/08/P08010, arXiv:1502.02702.

[53] CMS Collaboration, "Jet energy scale and resolution in the CMS experiment in pp collisions at 8 TeV", *JINST* **12** (2017) P02014, doi:10.1088/1748-0221/12/02/P02014, arXiv:1607.03663.

[54] D. Bertolini, P. Harris, M. Low, and N. Tran, "Pileup per particle identification", *JHEP* **10** (2014) 059, doi:10.1007/JHEP10(2014)059, arXiv:1407.6013.

[55] CMS Collaboration, "Pileup mitigation at CMS in 13 TeV data", *JINST* **15** (2020) P09018, doi:10.1088/1748-0221/15/09/p09018, arXiv:2003.00503.

[56] CMS Collaboration, "Jet performance in pp collisions at $\sqrt{s} = 7$ TeV", CMS Physics Analysis Summary CMS-PAS-JME-10-003, 2010.

[57] CMS Collaboration, "Jet algorithms performance in 13 TeV data", CMS Physics Analysis Summary CMS-PAS-JME-16-003, 2017.

[58] M. Dasgupta, A. Fregoso, S. Marzani, and G. P. Salam, "Towards an understanding of jet substructure", *JHEP* **09** (2013) 029, doi:10.1007/JHEP09(2013)029, arXiv:1307.0007.

[59] A. J. Larkoski, S. Marzani, G. Soyez, and J. Thaler, "Soft drop", *JHEP* **05** (2014) 146, doi:10.1007/JHEP05(2014)146, arXiv:1402.2657.

[60] CMS Collaboration, "Identification of heavy, energetic, hadronically decaying particles using machine-learning techniques", *JINST* **15** (Jun, 2020) P06005, doi:10.1088/1748-0221/15/06/p06005, arXiv:2004.08262.

[61] J. Thaler and K. Van Tilburg, "Identifying boosted objects with N-subjettiness", *JHEP* **03** (2011) 015, doi:10.1007/JHEP03(2011)015, arXiv:1011.2268.

[62] CMS Collaboration, "Identification of heavy-flavour jets with the CMS detector in pp collisions at 13 TeV", *JINST* **13** (2018) P05011, doi:10.1088/1748-0221/13/05/P05011, arXiv:1712.07158.

[63] CMS Collaboration, "Performance of missing transverse momentum reconstruction in proton-proton collisions at $\sqrt{s} = 13$ TeV using the CMS detector", *JINST* **14** (2019) P07004, doi:10.1088/1748-0221/14/07/P07004, arXiv:1903.06078.

[64] CMS Collaboration, "Precision luminosity measurement in proton-proton collisions at $\sqrt{s} = 13$ TeV in 2015 and 2016 at CMS", 2021. arXiv:2104.01927. Accepted by *Eur. Phys. J. C*.

[65] CMS Collaboration, "CMS luminosity measurement for the 2017 data-taking period at $\sqrt{s}$ = 13 TeV", cms physics analysis summary, 2018.

[66] CMS Collaboration, "CMS luminosity measurement for the 2018 data-taking period at $\sqrt{s}$ = 13 TeV", cms physics analysis summary, 2019.

[67] P. Vischia, "Reporting results in high energy physics publications: A manifesto", *Rev. Phys.* **5** (2020) 100046, doi:10.1016/j.revip.2020.100046, arXiv:1904.11718.

[68] A. L. Read, "Presentation of search results: the CL_s technique", *J. Phys. G* **28** (2002) 2693, doi:10.1088/0954-3899/28/10/313.

[69] G. Cowan, K. Cranmer, E. Gross, and O. Vitells, "Asymptotic formulae for likelihood-based tests of new physics", *Eur. Phys. J. C* **71** (2011) 1554, doi:10.1140/epjc/s10052-011-1554-0, arXiv:1007.1727. [Erratum: doi:10.1140/epjc/s10052-013-2501-z].

A The CMS Collaboration

Yerevan Physics Institute, Yerevan, Armenia
A. Tumasyan

Institut für Hochenergiephysik, Vienna, Austria
W. Adam, J.W. Andrejkovic, T. Bergauer, S. Chatterjee, M. Dragicevic, A. Escalante Del Valle, R. Frühwirth[1], M. Jeitler[1], N. Krammer, L. Lechner, D. Liko, I. Mikulec, P. Paulitsch, F.M. Pitters, J. Schieck[1], R. Schöfbeck, M. Spanring, S. Templ, W. Waltenberger, C.-E. Wulz[1]

Institute for Nuclear Problems, Minsk, Belarus
V. Chekhovsky, A. Litomin, V. Makarenko

Universiteit Antwerpen, Antwerpen, Belgium
M.R. Darwish[2], E.A. De Wolf, X. Janssen, T. Kello[3], A. Lelek, H. Rejeb Sfar, P. Van Mechelen, S. Van Putte, N. Van Remortel

Vrije Universiteit Brussel, Brussel, Belgium
F. Blekman, E.S. Bols, J. D'Hondt, J. De Clercq, M. Delcourt, H. El Faham, S. Lowette, S. Moortgat, A. Morton, D. Müller, A.R. Sahasransu, S. Tavernier, W. Van Doninck, P. Van Mulders

Université Libre de Bruxelles, Bruxelles, Belgium
D. Beghin, B. Bilin, B. Clerbaux, G. De Lentdecker, L. Favart, A. Grebenyuk, A.K. Kalsi, K. Lee, M. Mahdavikhorrami, I. Makarenko, L. Moureaux, L. Pétré, A. Popov, N. Postiau, E. Starling, L. Thomas, M. Vanden Bemden, C. Vander Velde, P. Vanlaer, D. Vannerom, L. Wezenbeek

Ghent University, Ghent, Belgium
T. Cornelis, D. Dobur, J. Knolle, L. Lambrecht, G. Mestdach, M. Niedziela, C. Roskas, A. Samalan, K. Skovpen, M. Tytgat, W. Verbeke, B. Vermassen, M. Vit

Université Catholique de Louvain, Louvain-la-Neuve, Belgium
A. Bethani, G. Bruno, F. Bury, C. Caputo, P. David, C. Delaere, I.S. Donertas, A. Giammanco, K. Jaffel, Sa. Jain, V. Lemaitre, K. Mondal, J. Prisciandaro, A. Taliercio, M. Teklishyn, T.T. Tran, P. Vischia, S. Wertz

Centro Brasileiro de Pesquisas Fisicas, Rio de Janeiro, Brazil
G.A. Alves, C. Hensel, A. Moraes

Universidade do Estado do Rio de Janeiro, Rio de Janeiro, Brazil
W.L. Aldá Júnior, M. Alves Gallo Pereira, M. Barroso Ferreira Filho, H. BRANDAO MALBOUISSON, W. Carvalho, J. Chinellato[4], E.M. Da Costa, G.G. Da Silveira[5], D. De Jesus Damiao, S. Fonseca De Souza, D. Matos Figueiredo, C. Mora Herrera, K. Mota Amarilo, L. Mundim, H. Nogima, P. Rebello Teles, A. Santoro, S.M. Silva Do Amaral, A. Sznajder, M. Thiel, F. Torres Da Silva De Araujo, A. Vilela Pereira

Universidade Estadual Paulista [a], Universidade Federal do ABC [b], São Paulo, Brazil
C.A. Bernardes[a,a,5], L. Calligaris[a], T.R. Fernandez Perez Tomei[a], E.M. Gregores[a,b], D.S. Lemos[a], P.G. Mercadante[a,b], S.F. Novaes[a], Sandra S. Padula[a]

Institute for Nuclear Research and Nuclear Energy, Bulgarian Academy of Sciences, Sofia, Bulgaria
A. Aleksandrov, G. Antchev, R. Hadjiiska, P. Iaydjiev, M. Misheva, M. Rodozov, M. Shopova, G. Sultanov

University of Sofia, Sofia, Bulgaria
A. Dimitrov, T. Ivanov, L. Litov, B. Pavlov, P. Petkov, A. Petrov

Beihang University, Beijing, China
T. Cheng, Q. Guo, T. Javaid[6], M. Mittal, H. Wang, L. Yuan

Department of Physics, Tsinghua University
M. Ahmad, G. Bauer, C. Dozen[7], Z. Hu, J. Martins[8], Y. Wang, K. Yi[9,10]

Institute of High Energy Physics, Beijing, China
E. Chapon, G.M. Chen[6], H.S. Chen[6], M. Chen, F. Iemmi, A. Kapoor, D. Leggat, H. Liao, Z.-A. LIU[6], V. Milosevic, F. Monti, R. Sharma, J. Tao, J. Thomas-wilsker, J. Wang, H. Zhang, S. Zhang[6], J. Zhao

State Key Laboratory of Nuclear Physics and Technology, Peking University, Beijing, China
A. Agapitos, Y. An, Y. Ban, C. Chen, A. Levin, Q. Li, X. Lyu, Y. Mao, S.J. Qian, D. Wang, Q. Wang, J. Xiao

Sun Yat-Sen University, Guangzhou, China
M. Lu, Z. You

Institute of Modern Physics and Key Laboratory of Nuclear Physics and Ion-beam Application (MOE) - Fudan University, Shanghai, China
X. Gao[3], H. Okawa

Zhejiang University, Hangzhou, China
Z. Lin, M. Xiao

Universidad de Los Andes, Bogota, Colombia
C. Avila, A. Cabrera, C. Florez, J. Fraga, A. Sarkar, M.A. Segura Delgado

Universidad de Antioquia, Medellin, Colombia
J. Mejia Guisao, F. Ramirez, J.D. Ruiz Alvarez, C.A. Salazar González

University of Split, Faculty of Electrical Engineering, Mechanical Engineering and Naval Architecture, Split, Croatia
D. Giljanovic, N. Godinovic, D. Lelas, I. Puljak

University of Split, Faculty of Science, Split, Croatia
Z. Antunovic, M. Kovac, T. Sculac

Institute Rudjer Boskovic, Zagreb, Croatia
V. Brigljevic, D. Ferencek, D. Majumder, M. Roguljic, A. Starodumov[11], T. Susa

University of Cyprus, Nicosia, Cyprus
A. Attikis, K. Christoforou, E. Erodotou, A. Ioannou, G. Kole, M. Kolosova, S. Konstantinou, J. Mousa, C. Nicolaou, F. Ptochos, P.A. Razis, H. Rykaczewski, H. Saka

Charles University, Prague, Czech Republic
M. Finger[12], M. Finger Jr.[12], A. Kveton

Escuela Politecnica Nacional, Quito, Ecuador
E. Ayala

Universidad San Francisco de Quito, Quito, Ecuador
E. Carrera Jarrin

Academy of Scientific Research and Technology of the Arab Republic of Egypt, Egyptian Network of High Energy Physics, Cairo, Egypt
H. Abdalla[13], A. Ellithi Kamel[13]

Center for High Energy Physics (CHEP-FU), Fayoum University, El-Fayoum, Egypt
M.A. Mahmoud, Y. Mohammed

National Institute of Chemical Physics and Biophysics, Tallinn, Estonia
S. Bhowmik, R.K. Dewanjee, K. Ehataht, M. Kadastik, S. Nandan, C. Nielsen, J. Pata, M. Raidal, L. Tani, C. Veelken

Department of Physics, University of Helsinki, Helsinki, Finland
P. Eerola, L. Forthomme, H. Kirschenmann, K. Osterberg, M. Voutilainen

Helsinki Institute of Physics, Helsinki, Finland
S. Bharthuar, E. Brücken, F. Garcia, J. Havukainen, M.S. Kim, R. Kinnunen, T. Lampén, K. Lassila-Perini, S. Lehti, T. Lindén, M. Lotti, L. Martikainen, M. Myllymäki, J. Ott, H. Siikonen, E. Tuominen, J. Tuominiemi

Lappeenranta University of Technology, Lappeenranta, Finland
P. Luukka, H. Petrow, T. Tuuva

IRFU, CEA, Université Paris-Saclay, Gif-sur-Yvette, France
C. Amendola, M. Besancon, F. Couderc, M. Dejardin, D. Denegri, J.L. Faure, F. Ferri, S. Ganjour, A. Givernaud, P. Gras, G. Hamel de Monchenault, P. Jarry, B. Lenzi, E. Locci, J. Malcles, J. Rander, A. Rosowsky, M.Ö. Sahin, A. Savoy-Navarro[14], M. Titov, G.B. Yu

Laboratoire Leprince-Ringuet, CNRS/IN2P3, Ecole Polytechnique, Institut Polytechnique de Paris, Palaiseau, France
S. Ahuja, F. Beaudette, M. Bonanomi, A. Buchot Perraguin, P. Busson, A. Cappati, C. Charlot, O. Davignon, B. Diab, G. Falmagne, S. Ghosh, R. Granier de Cassagnac, A. Hakimi, I. Kucher, J. Motta, M. Nguyen, C. Ochando, P. Paganini, J. Rembser, R. Salerno, J.B. Sauvan, Y. Sirois, A. Tarabini, A. Zabi, A. Zghiche

Université de Strasbourg, CNRS, IPHC UMR 7178, Strasbourg, France
J.-L. Agram[15], J. Andrea, D. Apparu, D. Bloch, G. Bourgatte, J.-M. Brom, E.C. Chabert, C. Collard, D. Darej, J.-C. Fontaine[15], U. Goerlach, C. Grimault, A.-C. Le Bihan, E. Nibigira, P. Van Hove

Institut de Physique des 2 Infinis de Lyon (IP2I), Villeurbanne, France
E. Asilar, S. Beauceron, C. Bernet, G. Boudoul, C. Camen, A. Carle, N. Chanon, D. Contardo, P. Depasse, H. El Mamouni, J. Fay, S. Gascon, M. Gouzevitch, B. Ille, I.B. Laktineh, H. Lattaud, A. Lesauvage, M. Lethuillier, L. Mirabito, S. Perries, K. Shchablo, V. Sordini, L. Torterotot, G. Touquet, M. Vander Donckt, S. Viret

Georgian Technical University, Tbilisi, Georgia
G. Adamov, I. Lomidze, Z. Tsamalaidze[12]

RWTH Aachen University, I. Physikalisches Institut, Aachen, Germany
L. Feld, K. Klein, M. Lipinski, D. Meuser, A. Pauls, M.P. Rauch, N. Röwert, J. Schulz, M. Teroerde

RWTH Aachen University, III. Physikalisches Institut A, Aachen, Germany
A. Dodonova, D. Eliseev, M. Erdmann, P. Fackeldey, B. Fischer, S. Ghosh, T. Hebbeker, K. Hoepfner, F. Ivone, H. Keller, L. Mastrolorenzo, M. Merschmeyer, A. Meyer, G. Mocellin,

S. Mondal, S. Mukherjee, D. Noll, A. Novak, T. Pook, A. Pozdnyakov, Y. Rath, H. Reithler, J. Roemer, A. Schmidt, S.C. Schuler, A. Sharma, L. Vigilante, S. Wiedenbeck, S. Zaleski

RWTH Aachen University, III. Physikalisches Institut B, Aachen, Germany
C. Dziwok, G. Flügge, W. Haj Ahmad[16], O. Hlushchenko, T. Kress, A. Nowack, C. Pistone, O. Pooth, D. Roy, H. Sert, A. Stahl[17], T. Ziemons

Deutsches Elektronen-Synchrotron, Hamburg, Germany
H. Aarup Petersen, M. Aldaya Martin, P. Asmuss, I. Babounikau, S. Baxter, O. Behnke, A. Bermúdez Martínez, S. Bhattacharya, A.A. Bin Anuar, K. Borras[18], V. Botta, D. Brunner, A. Campbell, A. Cardini, C. Cheng, F. Colombina, S. Consuegra Rodríguez, G. Correia Silva, V. Danilov, L. Didukh, G. Eckerlin, D. Eckstein, L.I. Estevez Banos, O. Filatov, E. Gallo[19], A. Geiser, A. Giraldi, A. Grohsjean, M. Guthoff, A. Jafari[20], N.Z. Jomhari, H. Jung, A. Kasem[18], M. Kasemann, H. Kaveh, C. Kleinwort, D. Krücker, W. Lange, J. Lidrych, K. Lipka, W. Lohmann[21], R. Mankel, I.-A. Melzer-Pellmann, M. Mendizabal Morentin, J. Metwally, A.B. Meyer, M. Meyer, J. Mnich, A. Mussgiller, Y. Otarid, D. Pérez Adán, D. Pitzl, A. Raspereza, B. Ribeiro Lopes, J. Rübenach, A. Saggio, A. Saibel, M. Savitskyi, M. Scham, V. Scheurer, P. Schütze, C. Schwanenberger[19], A. Singh, R.E. Sosa Ricardo, D. Stafford, N. Tonon, O. Turkot, M. Van De Klundert, R. Walsh, D. Walter, Y. Wen, K. Wichmann, L. Wiens, C. Wissing, S. Wuchterl

University of Hamburg, Hamburg, Germany
R. Aggleton, S. Albrecht, S. Bein, L. Benato, A. Benecke, P. Connor, K. De Leo, M. Eich, F. Feindt, A. Fröhlich, C. Garbers, E. Garutti, P. Gunnellini, J. Haller, A. Hinzmann, G. Kasieczka, R. Klanner, R. Kogler, T. Kramer, V. Kutzner, J. Lange, T. Lange, A. Lobanov, A. Malara, A. Nigamova, K.J. Pena Rodriguez, O. Rieger, P. Schleper, M. Schröder, J. Schwandt, D. Schwarz, J. Sonneveld, H. Stadie, G. Steinbrück, A. Tews, B. Vormwald, I. Zoi

Karlsruher Institut fuer Technologie, Karlsruhe, Germany
J. Bechtel, T. Berger, E. Butz, R. Caspart, T. Chwalek, W. De Boer[†], A. Dierlamm, A. Droll, K. El Morabit, N. Faltermann, M. Giffels, J.o. Gosewisch, A. Gottmann, F. Hartmann[17], C. Heidecker, U. Husemann, I. Katkov[22], P. Keicher, R. Koppenhöfer, S. Maier, M. Metzler, S. Mitra, Th. Müller, M. Neukum, A. Nürnberg, G. Quast, K. Rabbertz, J. Rauser, D. Savoiu, M. Schnepf, D. Seith, I. Shvetsov, H.J. Simonis, R. Ulrich, J. Van Der Linden, R.F. Von Cube, M. Wassmer, M. Weber, S. Wieland, R. Wolf, S. Wozniewski, S. Wunsch

Institute of Nuclear and Particle Physics (INPP), NCSR Demokritos, Aghia Paraskevi, Greece
G. Anagnostou, G. Daskalakis, T. Geralis, A. Kyriakis, D. Loukas, A. Stakia

National and Kapodistrian University of Athens, Athens, Greece
M. Diamantopoulou, D. Karasavvas, G. Karathanasis, P. Kontaxakis, C.K. Koraka, A. Manousakis-katsikakis, A. Panagiotou, I. Papavergou, N. Saoulidou, K. Theofilatos, E. Tziaferi, K. Vellidis, E. Vourliotis

National Technical University of Athens, Athens, Greece
G. Bakas, K. Kousouris, I. Papakrivopoulos, G. Tsipolitis, A. Zacharopoulou

University of Ioánnina, Ioánnina, Greece
I. Evangelou, C. Foudas, P. Gianneios, P. Katsoulis, P. Kokkas, N. Manthos, I. Papadopoulos, J. Strologas

MTA-ELTE Lendület CMS Particle and Nuclear Physics Group, Eötvös Loránd University

M. Csanad, K. Farkas, M.M.A. Gadallah[23], S. Lökös[24], P. Major, K. Mandal, A. Mehta, G. Pasztor, A.J. Rádl, O. Surányi, G.I. Veres

Wigner Research Centre for Physics, Budapest, Hungary
M. Bartók[25], G. Bencze, C. Hajdu, D. Horvath[26], F. Sikler, V. Veszpremi, G. Vesztergombi[†]

Institute of Nuclear Research ATOMKI, Debrecen, Hungary
S. Czellar, J. Karancsi[25], J. Molnar, Z. Szillasi, D. Teyssier

Institute of Physics, University of Debrecen
P. Raics, Z.L. Trocsanyi[27], B. Ujvari

Karoly Robert Campus, MATE Institute of Technology
T. Csorgo[28], F. Nemes[28], T. Novak

Indian Institute of Science (IISc), Bangalore, India
J.R. Komaragiri, D. Kumar, L. Panwar, P.C. Tiwari

National Institute of Science Education and Research, HBNI, Bhubaneswar, India
S. Bahinipati[29], C. Kar, P. Mal, T. Mishra, V.K. Muraleedharan Nair Bindhu[30], A. Nayak[30], P. Saha, N. Sur, S.K. Swain, D. Vats[30]

Panjab University, Chandigarh, India
S. Bansal, S.B. Beri, V. Bhatnagar, G. Chaudhary, S. Chauhan, N. Dhingra[31], R. Gupta, A. Kaur, M. Kaur, S. Kaur, P. Kumari, M. Meena, K. Sandeep, J.B. Singh, A.K. Virdi

University of Delhi, Delhi, India
A. Ahmed, A. Bhardwaj, B.C. Choudhary, M. Gola, S. Keshri, A. Kumar, M. Naimuddin, P. Priyanka, K. Ranjan, A. Shah

Saha Institute of Nuclear Physics, HBNI, Kolkata, India
M. Bharti[32], R. Bhattacharya, S. Bhattacharya, D. Bhowmik, S. Dutta, S. Dutta, B. Gomber[33], M. Maity[34], P. Palit, P.K. Rout, G. Saha, B. Sahu, S. Sarkar, M. Sharan, B. Singh[32], S. Thakur[32]

Indian Institute of Technology Madras, Madras, India
P.K. Behera, S.C. Behera, P. Kalbhor, A. Muhammad, R. Pradhan, P.R. Pujahari, A. Sharma, A.K. Sikdar

Bhabha Atomic Research Centre, Mumbai, India
D. Dutta, V. Jha, V. Kumar, D.K. Mishra, K. Naskar[35], P.K. Netrakanti, L.M. Pant, P. Shukla

Tata Institute of Fundamental Research-A, Mumbai, India
T. Aziz, S. Dugad, M. Kumar, U. Sarkar

Tata Institute of Fundamental Research-B, Mumbai, India
S. Banerjee, R. Chudasama, M. Guchait, S. Karmakar, S. Kumar, G. Majumder, K. Mazumdar, S. Mukherjee

Indian Institute of Science Education and Research (IISER), Pune, India
K. Alpana, S. Dube, B. Kansal, A. Laha, S. Pandey, A. Rane, A. Rastogi, S. Sharma

Isfahan University of Technology, Isfahan, Iran
H. Bakhshiansohi[36], M. Zeinali[37]

Institute for Research in Fundamental Sciences (IPM), Tehran, Iran
S. Chenarani[38], S.M. Etesami, M. Khakzad, M. Mohammadi Najafabadi

University College Dublin, Dublin, Ireland
M. Grunewald

INFN Sezione di Bari [a], Università di Bari [b], Politecnico di Bari [c], Bari, Italy
M. Abbrescia[a,b], R. Aly[a,b,39], C. Aruta[a,b], A. Colaleo[a], D. Creanza[a,c], N. De Filippis[a,c], M. De Palma[a,b], A. Di Florio[a,b], A. Di Pilato[a,b], W. Elmetenawee[a,b], L. Fiore[a], A. Gelmi[a,b], M. Gul[a], G. Iaselli[a,c], M. Ince[a,b], S. Lezki[a,b], G. Maggi[a,c], M. Maggi[a], I. Margjeka[a,b], V. Mastrapasqua[a,b], J.A. Merlin[a], S. My[a,b], S. Nuzzo[a,b], A. Pellecchia[a,b], A. Pompili[a,b], G. Pugliese[a,c], A. Ranieri[a], G. Selvaggi[a,b], L. Silvestris[a], F.M. Simone[a,b], R. Venditti[a], P. Verwilligen[a]

INFN Sezione di Bologna [a], Università di Bologna [b], Bologna, Italy
G. Abbiendi[a], C. Battilana[a,b], D. Bonacorsi[a,b], L. Borgonovi[a], L. Brigliadori[a], R. Campanini[a,b], P. Capiluppi[a,b], A. Castro[a,b], F.R. Cavallo[a], M. Cuffiani[a,b], G.M. Dallavalle[a], T. Diotalevi[a,b], F. Fabbri[a], A. Fanfani[a,b], P. Giacomelli[a], L. Giommi[a,b], C. Grandi[a], L. Guiducci[a,b], S. Lo Meo[a,40], L. Lunerti[a,b], S. Marcellini[a], G. Masetti[a], F.L. Navarria[a,b], A. Perrotta[a], F. Primavera[a,b], A.M. Rossi[a,b], T. Rovelli[a,b], G.P. Siroli[a,b]

INFN Sezione di Catania [a], Università di Catania [b], Catania, Italy
S. Albergo[a,b,41], S. Costa[a,b,41], A. Di Mattia[a], R. Potenza[a,b], A. Tricomi[a,b,41], C. Tuve[a,b]

INFN Sezione di Firenze [a], Università di Firenze [b], Firenze, Italy
G. Barbagli[a], A. Cassese[a], R. Ceccarelli[a,b], V. Ciulli[a,b], C. Civinini[a], R. D'Alessandro[a,b], E. Focardi[a,b], G. Latino[a,b], P. Lenzi[a,b], M. Lizzo[a,b], M. Meschini[a], S. Paoletti[a], R. Seidita[a,b], G. Sguazzoni[a], L. Viliani[a]

INFN Laboratori Nazionali di Frascati, Frascati, Italy
L. Benussi, S. Bianco, D. Piccolo

INFN Sezione di Genova [a], Università di Genova [b], Genova, Italy
M. Bozzo[a,b], F. Ferro[a], R. Mulargia[a,b], E. Robutti[a], S. Tosi[a,b]

INFN Sezione di Milano-Bicocca [a], Università di Milano-Bicocca [b], Milano, Italy
A. Benaglia[a], F. Brivio[a,b], F. Cetorelli[a,b], V. Ciriolo[a,b,17], F. De Guio[a,b], M.E. Dinardo[a,b], P. Dini[a], S. Gennai[a], A. Ghezzi[a,b], P. Govoni[a,b], L. Guzzi[a,b], M. Malberti[a], S. Malvezzi[a], A. Massironi[a], D. Menasce[a], L. Moroni[a], M. Paganoni[a,b], D. Pedrini[a], S. Ragazzi[a,b], N. Redaelli[a], T. Tabarelli de Fatis[a,b], D. Valsecchi[a,b,17], D. Zuolo[a,b]

INFN Sezione di Napoli [a], Università di Napoli 'Federico II' [b], Napoli, Italy, Università della Basilicata [c], Potenza, Italy, Università G. Marconi [d], Roma, Italy
S. Buontempo[a], F. Carnevali[a,b], N. Cavallo[a,c], A. De Iorio[a,b], F. Fabozzi[a,c], A.O.M. Iorio[a,b], L. Lista[a,b], S. Meola[a,d,17], P. Paolucci[a,17], B. Rossi[a], C. Sciacca[a,b]

INFN Sezione di Padova [a], Università di Padova [b], Padova, Italy, Università di Trento [c], Trento, Italy
P. Azzi[a], N. Bacchetta[a], D. Bisello[a,b], P. Bortignon[a], A. Bragagnolo[a,b], R. Carlin[a,b], P. Checchia[a], T. Dorigo[a], U. Dosselli[a], F. Gasparini[a,b], U. Gasparini[a,b], S.Y. Hoh[a,b], L. Layer[a,42], M. Margoni[a,b], A.T. Meneguzzo[a,b], J. Pazzini[a,b], M. Presilla[a,b], P. Ronchese[a,b], R. Rossin[a,b], F. Simonetto[a,b], G. Strong[a], M. Tosi[a,b], H. YARAR[a,b], M. Zanetti[a,b], P. Zotto[a,b], A. Zucchetta[a,b], G. Zumerle[a,b]

INFN Sezione di Pavia [a], Università di Pavia [b]
C. Aime'[a,b], A. Braghieri[a], S. Calzaferri[a,b], D. Fiorina[a,b], P. Montagna[a,b], S.P. Ratti[a,b], V. Re[a], C. Riccardi[a,b], P. Salvini[a], I. Vai[a], P. Vitulo[a,b]

INFN Sezione di Perugia [a], Università di Perugia [b], Perugia, Italy
P. Asenov[a,43], G.M. Bilei[a], D. Ciangottini[a,b], L. Fanò[a,b], P. Lariccia[a,b], M. Magherini[b], G. Mantovani[a,b], V. Mariani[a,b], M. Menichelli[a], F. Moscatelli[a,43], A. Piccinelli[a,b], A. Rossi[a,b], A. Santocchia[a,b], D. Spiga[a], T. Tedeschi[a,b]

INFN Sezione di Pisa [a], Università di Pisa [b], Scuola Normale Superiore di Pisa [c], Pisa Italy, Università di Siena [d], Siena, Italy
P. Azzurri[a], G. Bagliesi[a], V. Bertacchi[a,c], L. Bianchini[a], T. Boccali[a], E. Bossini[a,b], R. Castaldi[a], M.A. Ciocci[a,b], V. D'Amante[a,d], R. Dell'Orso[a], M.R. Di Domenico[a,d], S. Donato[a], A. Giassi[a], F. Ligabue[a,c], E. Manca[a,c], G. Mandorli[a,c], A. Messineo[a,b], F. Palla[a], S. Parolia[a,b], G. Ramirez-Sanchez[a,c], A. Rizzi[a,b], G. Rolandi[a,c], S. Roy Chowdhury[a,c], A. Scribano[a], N. Shafiei[a,b], P. Spagnolo[a], R. Tenchini[a], G. Tonelli[a,b], N. Turini[a,d], A. Venturi[a], P.G. Verdini[a]

INFN Sezione di Roma [a], Sapienza Università di Roma [b], Rome, Italy
M. Campana[a,b], F. Cavallari[a], D. Del Re[a,b], E. Di Marco[a], M. Diemoz[a], E. Longo[a,b], P. Meridiani[a], G. Organtini[a,b], F. Pandolfi[a], R. Paramatti[a,b], C. Quaranta[a,b], S. Rahatlou[a,b], C. Rovelli[a], F. Santanastasio[a,b], L. Soffi[a], R. Tramontano[a,b]

INFN Sezione di Torino [a], Università di Torino [b], Torino, Italy, Università del Piemonte Orientale [c], Novara, Italy
N. Amapane[a,b], R. Arcidiacono[a,c], S. Argiro[a,b], M. Arneodo[a,c], N. Bartosik[a], R. Bellan[a,b], A. Bellora[a,b], J. Berenguer Antequera[a,b], C. Biino[a], N. Cartiglia[a], S. Cometti[a], M. Costa[a,b], R. Covarelli[a,b], N. Demaria[a], B. Kiani[a,b], F. Legger[a], C. Mariotti[a], S. Maselli[a], E. Migliore[a,b], E. Monteil[a,b], M. Monteno[a], M.M. Obertino[a,b], G. Ortona[a], L. Pacher[a,b], N. Pastrone[a], M. Pelliccioni[a], G.L. Pinna Angioni[a,b], M. Ruspa[a,c], K. Shchelina[a,b], F. Siviero[a,b], V. Sola[a], A. Solano[a,b], D. Soldi[a,b], A. Staiano[a], M. Tornago[a,b], D. Trocino[a,b], A. Vagnerini

INFN Sezione di Trieste [a], Università di Trieste [b], Trieste, Italy
S. Belforte[a], V. Candelise[a,b], M. Casarsa[a], F. Cossutti[a], A. Da Rold[a,b], G. Della Ricca[a,b], G. Sorrentino[a,b], F. Vazzoler[a,b]

Kyungpook National University, Daegu, Korea
S. Dogra, C. Huh, B. Kim, D.H. Kim, G.N. Kim, J. Kim, J. Lee, S.W. Lee, C.S. Moon, Y.D. Oh, S.I. Pak, B.C. Radburn-Smith, S. Sekmen, Y.C. Yang

Chonnam National University, Institute for Universe and Elementary Particles, Kwangju, Korea
H. Kim, D.H. Moon

Hanyang University, Seoul, Korea
B. Francois, T.J. Kim, J. Park

Korea University, Seoul, Korea
S. Cho, S. Choi, Y. Go, B. Hong, K. Lee, K.S. Lee, J. Lim, J. Park, S.K. Park, J. Yoo

Kyung Hee University, Department of Physics, Seoul, Republic of Korea
J. Goh, A. Gurtu

Sejong University, Seoul, Korea
H.S. Kim, Y. Kim

Seoul National University, Seoul, Korea
J. Almond, J.H. Bhyun, J. Choi, S. Jeon, J. Kim, J.S. Kim, S. Ko, H. Kwon, H. Lee, S. Lee, B.H. Oh, M. Oh, S.B. Oh, H. Seo, U.K. Yang, I. Yoon

University of Seoul, Seoul, Korea
W. Jang, D. Jeon, D.Y. Kang, Y. Kang, J.H. Kim, S. Kim, B. Ko, J.S.H. Lee, Y. Lee, I.C. Park, Y. Roh, M.S. Ryu, D. Song, I.J. Watson, S. Yang

Yonsei University, Department of Physics, Seoul, Korea
S. Ha, H.D. Yoo

Sungkyunkwan University, Suwon, Korea
M. Choi, Y. Jeong, H. Lee, Y. Lee, I. Yu

College of Engineering and Technology, American University of the Middle East (AUM), Egaila, Kuwait
T. Beyrouthy, Y. Maghrbi

Riga Technical University
T. Torims, V. Veckalns[44]

Vilnius University, Vilnius, Lithuania
M. Ambrozas, A. Carvalho Antunes De Oliveira, A. Juodagalvis, A. Rinkevicius, G. Tamulaitis

National Centre for Particle Physics, Universiti Malaya, Kuala Lumpur, Malaysia
N. Bin Norjoharuddeen, W.A.T. Wan Abdullah, M.N. Yusli, Z. Zolkapli

Universidad de Sonora (UNISON), Hermosillo, Mexico
J.F. Benitez, A. Castaneda Hernandez, M. León Coello, J.A. Murillo Quijada, A. Sehrawat, L. Valencia Palomo

Centro de Investigacion y de Estudios Avanzados del IPN, Mexico City, Mexico
G. Ayala, H. Castilla-Valdez, E. De La Cruz-Burelo, I. Heredia-De La Cruz[45], R. Lopez-Fernandez, C.A. Mondragon Herrera, D.A. Perez Navarro, A. Sanchez-Hernandez

Universidad Iberoamericana, Mexico City, Mexico
S. Carrillo Moreno, C. Oropeza Barrera, M. Ramirez-Garcia, F. Vazquez Valencia

Benemerita Universidad Autonoma de Puebla, Puebla, Mexico
I. Pedraza, H.A. Salazar Ibarguen, C. Uribe Estrada

University of Montenegro, Podgorica, Montenegro
J. Mijuskovic[46], N. Raicevic

University of Auckland, Auckland, New Zealand
D. Krofcheck

University of Canterbury, Christchurch, New Zealand
S. Bheesette, P.H. Butler

National Centre for Physics, Quaid-I-Azam University, Islamabad, Pakistan
A. Ahmad, M.I. Asghar, A. Awais, M.I.M. Awan, H.R. Hoorani, W.A. Khan, M.A. Shah, M. Shoaib, M. Waqas

AGH University of Science and Technology Faculty of Computer Science, Electronics and Telecommunications, Krakow, Poland
V. Avati, L. Grzanka, M. Malawski

National Centre for Nuclear Research, Swierk, Poland
H. Bialkowska, M. Bluj, B. Boimska, M. Górski, M. Kazana, M. Szleper, P. Zalewski

Institute of Experimental Physics, Faculty of Physics, University of Warsaw, Warsaw, Poland
K. Bunkowski, K. Doroba, A. Kalinowski, M. Konecki, J. Krolikowski, M. Walczak

Laboratório de Instrumentação e Física Experimental de Partículas, Lisboa, Portugal
M. Araujo, P. Bargassa, D. Bastos, A. Boletti, P. Faccioli, M. Gallinaro, J. Hollar, N. Leonardo, T. Niknejad, M. Pisano, J. Seixas, O. Toldaiev, J. Varela

Joint Institute for Nuclear Research, Dubna, Russia
S. Afanasiev, D. Budkouski, I. Golutvin, I. Gorbunov, V. Karjavine, V. Korenkov, A. Lanev, A. Malakhov, V. Matveev[47,48], V. Palichik, V. Perelygin, M. Savina, D. Seitova, V. Shalaev, S. Shmatov, S. Shulha, V. Smirnov, O. Teryaev, N. Voytishin, B.S. Yuldashev[49], A. Zarubin, I. Zhizhin

Petersburg Nuclear Physics Institute, Gatchina (St. Petersburg), Russia
G. Gavrilov, V. Golovtcov, Y. Ivanov, V. Kim[50], E. Kuznetsova[51], V. Murzin, V. Oreshkin, I. Smirnov, D. Sosnov, V. Sulimov, L. Uvarov, S. Volkov, A. Vorobyev

Institute for Nuclear Research, Moscow, Russia
Yu. Andreev, A. Dermenev, S. Gninenko, N. Golubev, A. Karneyeu, D. Kirpichnikov, M. Kirsanov, N. Krasnikov, A. Pashenkov, G. Pivovarov, D. Tlisov[†], A. Toropin

Institute for Theoretical and Experimental Physics named by A.I. Alikhanov of NRC 'Kurchatov Institute', Moscow, Russia
V. Epshteyn, V. Gavrilov, N. Lychkovskaya, A. Nikitenko[52], V. Popov, A. Spiridonov, A. Stepennov, M. Toms, E. Vlasov, A. Zhokin

Moscow Institute of Physics and Technology, Moscow, Russia
T. Aushev

National Research Nuclear University 'Moscow Engineering Physics Institute' (MEPhI), Moscow, Russia
O. Bychkova, M. Chadeeva[53], P. Parygin, E. Popova, V. Rusinov

P.N. Lebedev Physical Institute, Moscow, Russia
V. Andreev, M. Azarkin, I. Dremin, M. Kirakosyan, A. Terkulov

Skobeltsyn Institute of Nuclear Physics, Lomonosov Moscow State University, Moscow, Russia
A. Belyaev, E. Boos, V. Bunichev, M. Dubinin[54], L. Dudko, A. Ershov, V. Klyukhin, O. Kodolova, I. Lokhtin, S. Obraztsov, M. Perfilov, S. Petrushanko, V. Savrin

Novosibirsk State University (NSU), Novosibirsk, Russia
V. Blinov[55], T. Dimova[55], L. Kardapoltsev[55], A. Kozyrev[55], I. Ovtin[55], Y. Skovpen[55]

Institute for High Energy Physics of National Research Centre 'Kurchatov Institute', Protvino, Russia
I. Azhgirey, I. Bayshev, D. Elumakhov, V. Kachanov, D. Konstantinov, P. Mandrik, V. Petrov, R. Ryutin, S. Slabospitskii, A. Sobol, S. Troshin, N. Tyurin, A. Uzunian, A. Volkov

National Research Tomsk Polytechnic University, Tomsk, Russia
A. Babaev, V. Okhotnikov

Tomsk State University, Tomsk, Russia
V. Borshch, V. Ivanchenko, E. Tcherniaev

University of Belgrade: Faculty of Physics and VINCA Institute of Nuclear Sciences, Belgrade, Serbia
P. Adzic[56], M. Dordevic, P. Milenovic, J. Milosevic

Centro de Investigaciones Energéticas Medioambientales y Tecnológicas (CIEMAT), Madrid, Spain
M. Aguilar-Benitez, J. Alcaraz Maestre, A. Álvarez Fernández, I. Bachiller, M. Barrio Luna, Cristina F. Bedoya, C.A. Carrillo Montoya, M. Cepeda, M. Cerrada, N. Colino, B. De La Cruz, A. Delgado Peris, J.P. Fernández Ramos, J. Flix, M.C. Fouz, O. Gonzalez Lopez, S. Goy Lopez, J.M. Hernandez, M.I. Josa, J. León Holgado, D. Moran, Á. Navarro Tobar, C. Perez Dengra, A. Pérez-Calero Yzquierdo, J. Puerta Pelayo, I. Redondo, L. Romero, S. Sánchez Navas, L. Urda Gómez, C. Willmott

Universidad Autónoma de Madrid, Madrid, Spain
J.F. de Trocóniz, R. Reyes-Almanza

Universidad de Oviedo, Instituto Universitario de Ciencias y Tecnologías Espaciales de Asturias (ICTEA), Oviedo, Spain
B. Alvarez Gonzalez, J. Cuevas, C. Erice, J. Fernandez Menendez, S. Folgueras, I. Gonzalez Caballero, J.R. González Fernández, E. Palencia Cortezon, C. Ramón Álvarez, J. Ripoll Sau, V. Rodríguez Bouza, A. Trapote, N. Trevisani

Instituto de Física de Cantabria (IFCA), CSIC-Universidad de Cantabria, Santander, Spain
J.A. Brochero Cifuentes, I.J. Cabrillo, A. Calderon, J. Duarte Campderros, M. Fernandez, C. Fernandez Madrazo, P.J. Fernández Manteca, A. García Alonso, G. Gomez, C. Martinez Rivero, P. Martinez Ruiz del Arbol, F. Matorras, P. Matorras Cuevas, J. Piedra Gomez, C. Prieels, T. Rodrigo, A. Ruiz-Jimeno, L. Scodellaro, I. Vila, J.M. Vizan Garcia

University of Colombo, Colombo, Sri Lanka
MK Jayananda, B. Kailasapathy[57], D.U.J. Sonnadara, DDC Wickramarathna

University of Ruhuna, Department of Physics, Matara, Sri Lanka
W.G.D. Dharmaratna, K. Liyanage, N. Perera, N. Wickramage

CERN, European Organization for Nuclear Research, Geneva, Switzerland
T.K. Aarrestad, D. Abbaneo, J. Alimena, E. Auffray, G. Auzinger, J. Baechler, P. Baillon†, D. Barney, J. Bendavid, M. Bianco, A. Bocci, T. Camporesi, M. Capeans Garrido, G. Cerminara, S.S. Chhibra, M. Cipriani, L. Cristella, D. d'Enterria, A. Dabrowski, N. Daci, A. David, A. De Roeck, M.M. Defranchis, M. Deile, M. Dobson, M. Dünser, N. Dupont, A. Elliott-Peisert, N. Emriskova, F. Fallavollita[58], D. Fasanella, A. Florent, G. Franzoni, W. Funk, S. Giani, D. Gigi, K. Gill, F. Glege, L. Gouskos, M. Haranko, J. Hegeman, Y. Iiyama, V. Innocente, T. James, P. Janot, J. Kaspar, J. Kieseler, M. Komm, N. Kratochwil, C. Lange, S. Laurila, P. Lecoq, K. Long, C. Lourenço, L. Malgeri, S. Mallios, M. Mannelli, A.C. Marini, F. Meijers, S. Mersi, E. Meschi, F. Moortgat, M. Mulders, S. Orfanelli, L. Orsini, F. Pantaleo, L. Pape, E. Perez, M. Peruzzi, A. Petrilli, G. Petrucciani, A. Pfeiffer, M. Pierini, D. Piparo, M. Pitt, H. Qu, T. Quast, D. Rabady, A. Racz, G. Reales Gutiérrez, M. Rieger, M. Rovere, H. Sakulin, J. Salfeld-Nebgen, S. Scarfi, C. Schäfer, C. Schwick, M. Selvaggi, A. Sharma, P. Silva, W. Snoeys, P. Sphicas[59], S. Summers, K. Tatar, V.R. Tavolaro, D. Treille, A. Tsirou, G.P. Van Onsem, M. Verzetti, J. Wanczyk[60], K.A. Wozniak, W.D. Zeuner

Paul Scherrer Institut, Villigen, Switzerland
L. Caminada[61], A. Ebrahimi, W. Erdmann, R. Horisberger, Q. Ingram, H.C. Kaestli, D. Kotlinski, U. Langenegger, M. Missiroli, T. Rohe

ETH Zurich - Institute for Particle Physics and Astrophysics (IPA), Zurich, Switzerland
K. Androsov[60], M. Backhaus, P. Berger, A. Calandri, N. Chernyavskaya, A. De Cosa, G. Dissertori, M. Dittmar, M. Donegà, C. Dorfer, F. Eble, K. Gedia, F. Glessgen, T.A. Gómez Espinosa, C. Grab, D. Hits, W. Lustermann, A.-M. Lyon, R.A. Manzoni, C. Martin Perez, M.T. Meinhard, F. Nessi-Tedaldi, J. Niedziela, F. Pauss, V. Perovic, S. Pigazzini, M.G. Ratti, M. Reichmann, C. Reissel, T. Reitenspiess, B. Ristic, D. Ruini, D.A. Sanz Becerra, M. Schönenberger, V. Stampf, J. Steggemann[60], R. Wallny, D.H. Zhu

Universität Zürich, Zurich, Switzerland
C. Amsler[62], P. Bärtschi, C. Botta, D. Brzhechko, M.F. Canelli, K. Cormier, A. De Wit, R. Del Burgo, J.K. Heikkilä, M. Huwiler, W. Jin, A. Jofrehei, B. Kilminster, S. Leontsinis, S.P. Liechti, A. Macchiolo, P. Meiring, V.M. Mikuni, U. Molinatti, I. Neutelings, A. Reimers, P. Robmann, S. Sanchez Cruz, K. Schweiger, Y. Takahashi

National Central University, Chung-Li, Taiwan
C. Adloff[63], C.M. Kuo, W. Lin, A. Roy, T. Sarkar[34], S.S. Yu

National Taiwan University (NTU), Taipei, Taiwan
L. Ceard, Y. Chao, K.F. Chen, P.H. Chen, W.-S. Hou, Y.y. Li, R.-S. Lu, E. Paganis, A. Psallidas, A. Steen, H.y. Wu, E. Yazgan, P.r. Yu

Chulalongkorn University, Faculty of Science, Department of Physics, Bangkok, Thailand
B. Asavapibhop, C. Asawatangtrakuldee, N. Srimanobhas

Çukurova University, Physics Department, Science and Art Faculty, Adana, Turkey
F. Boran, S. Damarseckin[64], Z.S. Demiroglu, F. Dolek, I. Dumanoglu[65], E. Eskut, Y. Guler, E. Gurpinar Guler[66], I. Hos[67], C. Isik, O. Kara, A. Kayis Topaksu, U. Kiminsu, G. Onengut, K. Ozdemir[68], A. Polatoz, A.E. Simsek, B. Tali[69], U.G. Tok, S. Turkcapar, I.S. Zorbakir, C. Zorbilmez

Middle East Technical University, Physics Department, Ankara, Turkey
B. Isildak[70], G. Karapinar[71], K. Ocalan[72], M. Yalvac[73]

Bogazici University, Istanbul, Turkey
B. Akgun, I.O. Atakisi, E. Gülmez, M. Kaya[74], O. Kaya[75], Ö. Özçelik, S. Tekten[76], E.A. Yetkin[77]

Istanbul Technical University, Istanbul, Turkey
A. Cakir, K. Cankocak[65], Y. Komurcu, S. Sen[78]

Istanbul University, Istanbul, Turkey
S. Cerci[69], B. Kaynak, S. Ozkorucuklu, D. Sunar Cerci[69]

Institute for Scintillation Materials of National Academy of Science of Ukraine, Kharkov, Ukraine
B. Grynyov

National Scientific Center, Kharkov Institute of Physics and Technology, Kharkov, Ukraine
L. Levchuk

University of Bristol, Bristol, United Kingdom
D. Anthony, E. Bhal, S. Bologna, J.J. Brooke, A. Bundock, E. Clement, D. Cussans, H. Flacher, J. Goldstein, G.P. Heath, H.F. Heath, M.l. Holmberg[79], L. Kreczko, B. Krikler, S. Paramesvaran, S. Seif El Nasr-Storey, V.J. Smith, N. Stylianou[80], K. Walkingshaw Pass, R. White

Rutherford Appleton Laboratory, Didcot, United Kingdom
K.W. Bell, A. Belyaev[81], C. Brew, R.M. Brown, D.J.A. Cockerill, C. Cooke, K.V. Ellis, K. Harder,

S. Harper, J. Linacre, K. Manolopoulos, D.M. Newbold, E. Olaiya, D. Petyt, T. Reis, T. Schuh, C.H. Shepherd-Themistocleous, I.R. Tomalin, T. Williams

Imperial College, London, United Kingdom
R. Bainbridge, P. Bloch, S. Bonomally, J. Borg, S. Breeze, O. Buchmuller, V. Cepaitis, G.S. Chahal[82], D. Colling, P. Dauncey, G. Davies, M. Della Negra, S. Fayer, G. Fedi, G. Hall, M.H. Hassanshahi, G. Iles, J. Langford, L. Lyons, A.-M. Magnan, S. Malik, A. Martelli, D.G. Monk, J. Nash[83], M. Pesaresi, D.M. Raymond, A. Richards, A. Rose, E. Scott, C. Seez, A. Shtipliyski, A. Tapper, K. Uchida, T. Virdee[17], M. Vojinovic, N. Wardle, S.N. Webb, D. Winterbottom, A.G. Zecchinelli

Brunel University, Uxbridge, United Kingdom
K. Coldham, J.E. Cole, A. Khan, P. Kyberd, I.D. Reid, L. Teodorescu, S. Zahid

Baylor University, Waco, USA
S. Abdullin, A. Brinkerhoff, B. Caraway, J. Dittmann, K. Hatakeyama, A.R. Kanuganti, B. McMaster, N. Pastika, M. Saunders, S. Sawant, C. Sutantawibul, J. Wilson

Catholic University of America, Washington, DC, USA
R. Bartek, A. Dominguez, R. Uniyal, A.M. Vargas Hernandez

The University of Alabama, Tuscaloosa, USA
A. Buccilli, S.I. Cooper, D. Di Croce, S.V. Gleyzer, C. Henderson, C.U. Perez, P. Rumerio[84], C. West

Boston University, Boston, USA
A. Akpinar, A. Albert, D. Arcaro, C. Cosby, Z. Demiragli, E. Fontanesi, D. Gastler, J. Rohlf, K. Salyer, D. Sperka, D. Spitzbart, I. Suarez, A. Tsatsos, S. Yuan, D. Zou

Brown University, Providence, USA
G. Benelli, B. Burkle, X. Coubez[18], D. Cutts, M. Hadley, U. Heintz, J.M. Hogan[85], G. Landsberg, K.T. Lau, M. Lukasik, J. Luo, M. Narain, S. Sagir[86], E. Usai, W.Y. Wong, X. Yan, D. Yu, W. Zhang

University of California, Davis, Davis, USA
J. Bonilla, C. Brainerd, R. Breedon, M. Calderon De La Barca Sanchez, M. Chertok, J. Conway, P.T. Cox, R. Erbacher, G. Haza, F. Jensen, O. Kukral, R. Lander, M. Mulhearn, D. Pellett, B. Regnery, D. Taylor, Y. Yao, F. Zhang

University of California, Los Angeles, USA
M. Bachtis, R. Cousins, A. Datta, D. Hamilton, J. Hauser, M. Ignatenko, M.A. Iqbal, T. Lam, W.A. Nash, S. Regnard, D. Saltzberg, B. Stone, V. Valuev

University of California, Riverside, Riverside, USA
K. Burt, Y. Chen, R. Clare, J.W. Gary, M. Gordon, G. Hanson, G. Karapostoli, O.R. Long, N. Manganelli, M. Olmedo Negrete, W. Si, S. Wimpenny, Y. Zhang

University of California, San Diego, La Jolla, USA
J.G. Branson, P. Chang, S. Cittolin, S. Cooperstein, N. Deelen, D. Diaz, J. Duarte, R. Gerosa, L. Giannini, D. Gilbert, J. Guiang, R. Kansal, V. Krutelyov, R. Lee, J. Letts, M. Masciovecchio, S. May, M. Pieri, B.V. Sathia Narayanan, V. Sharma, M. Tadel, A. Vartak, F. Würthwein, Y. Xiang, A. Yagil

University of California, Santa Barbara - Department of Physics, Santa Barbara, USA
N. Amin, C. Campagnari, M. Citron, A. Dorsett, V. Dutta, J. Incandela, M. Kilpatrick, J. Kim, B. Marsh, H. Mei, M. Oshiro, M. Quinnan, J. Richman, U. Sarica, J. Sheplock, D. Stuart, S. Wang

California Institute of Technology, Pasadena, USA
A. Bornheim, O. Cerri, I. Dutta, J.M. Lawhorn, N. Lu, J. Mao, H.B. Newman, T.Q. Nguyen, M. Spiropulu, J.R. Vlimant, C. Wang, S. Xie, Z. Zhang, R.Y. Zhu

Carnegie Mellon University, Pittsburgh, USA
J. Alison, S. An, M.B. Andrews, P. Bryant, T. Ferguson, A. Harilal, C. Liu, T. Mudholkar, M. Paulini, A. Sanchez, W. Terrill

University of Colorado Boulder, Boulder, USA
J.P. Cumalat, W.T. Ford, A. Hassani, E. MacDonald, R. Patel, A. Perloff, C. Savard, K. Stenson, K.A. Ulmer, S.R. Wagner

Cornell University, Ithaca, USA
J. Alexander, S. Bright-thonney, Y. Cheng, D.J. Cranshaw, S. Hogan, J. Monroy, J.R. Patterson, D. Quach, J. Reichert, M. Reid, A. Ryd, W. Sun, J. Thom, P. Wittich, R. Zou

Fermi National Accelerator Laboratory, Batavia, USA
M. Albrow, M. Alyari, G. Apollinari, A. Apresyan, A. Apyan, S. Banerjee, L.A.T. Bauerdick, D. Berry, J. Berryhill, P.C. Bhat, K. Burkett, J.N. Butler, A. Canepa, G.B. Cerati, H.W.K. Cheung, F. Chlebana, M. Cremonesi, K.F. Di Petrillo, V.D. Elvira, Y. Feng, J. Freeman, Z. Gecse, L. Gray, D. Green, S. Grünendahl, O. Gutsche, R.M. Harris, R. Heller, T.C. Herwig, J. Hirschauer, B. Jayatilaka, S. Jindariani, M. Johnson, U. Joshi, T. Klijnsma, B. Klima, K.H.M. Kwok, S. Lammel, D. Lincoln, R. Lipton, T. Liu, C. Madrid, K. Maeshima, C. Mantilla, D. Mason, P. McBride, P. Merkel, S. Mrenna, S. Nahn, J. Ngadiuba, V. O'Dell, V. Papadimitriou, K. Pedro, C. Pena[54], O. Prokofyev, F. Ravera, A. Reinsvold Hall, L. Ristori, B. Schneider, E. Sexton-Kennedy, N. Smith, A. Soha, W.J. Spalding, L. Spiegel, S. Stoynev, J. Strait, L. Taylor, S. Tkaczyk, N.V. Tran, L. Uplegger, E.W. Vaandering, H.A. Weber

University of Florida, Gainesville, USA
D. Acosta, P. Avery, D. Bourilkov, L. Cadamuro, V. Cherepanov, F. Errico, R.D. Field, D. Guerrero, B.M. Joshi, M. Kim, E. Koenig, J. Konigsberg, A. Korytov, K.H. Lo, K. Matchev, N. Menendez, G. Mitselmakher, A. Muthirakalayil Madhu, N. Rawal, D. Rosenzweig, S. Rosenzweig, K. Shi, J. Sturdy, J. Wang, E. Yigitbasi, X. Zuo

Florida State University, Tallahassee, USA
T. Adams, A. Askew, R. Habibullah, V. Hagopian, K.F. Johnson, R. Khurana, T. Kolberg, G. Martinez, H. Prosper, C. Schiber, O. Viazlo, R. Yohay, J. Zhang

Florida Institute of Technology, Melbourne, USA
M.M. Baarmand, S. Butalla, T. Elkafrawy[87], M. Hohlmann, R. Kumar Verma, D. Noonan, M. Rahmani, F. Yumiceva

University of Illinois at Chicago (UIC), Chicago, USA
M.R. Adams, H. Becerril Gonzalez, R. Cavanaugh, X. Chen, S. Dittmer, O. Evdokimov, C.E. Gerber, D.A. Hangal, D.J. Hofman, A.H. Merrit, C. Mills, G. Oh, T. Roy, S. Rudrabhatla, M.B. Tonjes, N. Varelas, J. Viinikainen, X. Wang, Z. Wu, Z. Ye

The University of Iowa, Iowa City, USA
M. Alhusseini, K. Dilsiz[88], R.P. Gandrajula, O.K. Köseyan, J.-P. Merlo, A. Mestvirishvili[89], J. Nachtman, H. Ogul[90], Y. Onel, A. Penzo, C. Snyder, E. Tiras[91]

Johns Hopkins University, Baltimore, USA
O. Amram, B. Blumenfeld, L. Corcodilos, J. Davis, M. Eminizer, A.V. Gritsan, S. Kyriacou, P. Maksimovic, J. Roskes, M. Swartz, T.Á. Vámi

The University of Kansas, Lawrence, USA
A. Abreu, J. Anguiano, C. Baldenegro Barrera, P. Baringer, A. Bean, A. Bylinkin, Z. Flowers, T. Isidori, S. Khalil, J. King, G. Krintiras, A. Kropivnitskaya, M. Lazarovits, C. Lindsey, J. Marquez, N. Minafra, M. Murray, M. Nickel, C. Rogan, C. Royon, R. Salvatico, S. Sanders, E. Schmitz, C. Smith, J.D. Tapia Takaki, Q. Wang, Z. Warner, J. Williams, G. Wilson

Kansas State University, Manhattan, USA
S. Duric, A. Ivanov, K. Kaadze, D. Kim, Y. Maravin, T. Mitchell, A. Modak, K. Nam

Lawrence Livermore National Laboratory, Livermore, USA
F. Rebassoo, D. Wright

University of Maryland, College Park, USA
E. Adams, A. Baden, O. Baron, A. Belloni, S.C. Eno, N.J. Hadley, S. Jabeen, R.G. Kellogg, T. Koeth, A.C. Mignerey, S. Nabili, C. Palmer, M. Seidel, A. Skuja, L. Wang, K. Wong

Massachusetts Institute of Technology, Cambridge, USA
D. Abercrombie, G. Andreassi, R. Bi, S. Brandt, W. Busza, I.A. Cali, Y. Chen, M. D'Alfonso, J. Eysermans, C. Freer, G. Gomez Ceballos, M. Goncharov, P. Harris, M. Hu, M. Klute, D. Kovalskyi, J. Krupa, Y.-J. Lee, B. Maier, C. Mironov, C. Paus, D. Rankin, C. Roland, G. Roland, Z. Shi, G.S.F. Stephans, J. Wang, Z. Wang, B. Wyslouch

University of Minnesota, Minneapolis, USA
R.M. Chatterjee, A. Evans, P. Hansen, J. Hiltbrand, Sh. Jain, M. Krohn, Y. Kubota, J. Mans, M. Revering, R. Rusack, R. Saradhy, N. Schroeder, N. Strobbe, M.A. Wadud

University of Nebraska-Lincoln, Lincoln, USA
K. Bloom, M. Bryson, S. Chauhan, D.R. Claes, C. Fangmeier, L. Finco, F. Golf, C. Joo, I. Kravchenko, M. Musich, I. Reed, J.E. Siado, G.R. Snow[†], W. Tabb, F. Yan

State University of New York at Buffalo, Buffalo, USA
G. Agarwal, H. Bandyopadhyay, L. Hay, I. Iashvili, A. Kharchilava, C. McLean, D. Nguyen, J. Pekkanen, S. Rappoccio, A. Williams

Northeastern University, Boston, USA
G. Alverson, E. Barberis, Y. Haddad, A. Hortiangtham, J. Li, G. Madigan, B. Marzocchi, D.M. Morse, V. Nguyen, T. Orimoto, A. Parker, L. Skinnari, A. Tishelman-Charny, T. Wamorkar, B. Wang, A. Wisecarver, D. Wood

Northwestern University, Evanston, USA
S. Bhattacharya, J. Bueghly, Z. Chen, A. Gilbert, T. Gunter, K.A. Hahn, Y. Liu, N. Odell, M.H. Schmitt, M. Velasco

University of Notre Dame, Notre Dame, USA
R. Band, R. Bucci, A. Das, N. Dev, R. Goldouzian, M. Hildreth, K. Hurtado Anampa, C. Jessop, K. Lannon, J. Lawrence, N. Loukas, D. Lutton, N. Marinelli, I. Mcalister, T. McCauley, C. Mcgrady, F. Meng, K. Mohrman, Y. Musienko[47], R. Ruchti, P. Siddireddy, A. Townsend, M. Wayne, A. Wightman, M. Wolf, M. Zarucki, L. Zygala

The Ohio State University, Columbus, USA
B. Bylsma, B. Cardwell, L.S. Durkin, B. Francis, C. Hill, M. Nunez Ornelas, K. Wei, B.L. Winer, B.R. Yates

Princeton University, Princeton, USA
F.M. Addesa, B. Bonham, P. Das, G. Dezoort, P. Elmer, A. Frankenthal, B. Greenberg,

N. Haubrich, S. Higginbotham, A. Kalogeropoulos, G. Kopp, S. Kwan, D. Lange, M.T. Lucchini, D. Marlow, K. Mei, I. Ojalvo, J. Olsen, D. Stickland, C. Tully

University of Puerto Rico, Mayaguez, USA
S. Malik, S. Norberg

Purdue University, West Lafayette, USA
A.S. Bakshi, V.E. Barnes, R. Chawla, S. Das, L. Gutay, M. Jones, A.W. Jung, S. Karmarkar, M. Liu, G. Negro, N. Neumeister, G. Paspalaki, C.C. Peng, S. Piperov, A. Purohit, J.F. Schulte, M. Stojanovic[14], J. Thieman, F. Wang, R. Xiao, W. Xie

Purdue University Northwest, Hammond, USA
J. Dolen, N. Parashar

Rice University, Houston, USA
A. Baty, M. Decaro, S. Dildick, K.M. Ecklund, S. Freed, P. Gardner, F.J.M. Geurts, A. Kumar, W. Li, B.P. Padley, R. Redjimi, W. Shi, A.G. Stahl Leiton, S. Yang, L. Zhang, Y. Zhang

University of Rochester, Rochester, USA
A. Bodek, P. de Barbaro, R. Demina, J.L. Dulemba, C. Fallon, T. Ferbel, M. Galanti, A. Garcia-Bellido, O. Hindrichs, A. Khukhunaishvili, E. Ranken, R. Taus

Rutgers, The State University of New Jersey, Piscataway, USA
B. Chiarito, J.P. Chou, A. Gandrakota, Y. Gershtein, E. Halkiadakis, A. Hart, M. Heindl, O. Karacheban[21], I. Laflotte, A. Lath, R. Montalvo, K. Nash, M. Osherson, S. Salur, S. Schnetzer, S. Somalwar, R. Stone, S.A. Thayil, S. Thomas, H. Wang

University of Tennessee, Knoxville, USA
H. Acharya, A.G. Delannoy, S. Fiorendi, S. Spanier

Texas A&M University, College Station, USA
O. Bouhali[92], M. Dalchenko, A. Delgado, R. Eusebi, J. Gilmore, T. Huang, T. Kamon[93], H. Kim, S. Luo, S. Malhotra, R. Mueller, D. Overton, D. Rathjens, A. Safonov

Texas Tech University, Lubbock, USA
N. Akchurin, J. Damgov, V. Hegde, S. Kunori, K. Lamichhane, S.W. Lee, T. Mengke, S. Muthumuni, T. Peltola, I. Volobouev, Z. Wang, A. Whitbeck

Vanderbilt University, Nashville, USA
E. Appelt, S. Greene, A. Gurrola, W. Johns, A. Melo, H. Ni, K. Padeken, F. Romeo, P. Sheldon, S. Tuo, J. Velkovska

University of Virginia, Charlottesville, USA
M.W. Arenton, B. Cox, G. Cummings, J. Hakala, R. Hirosky, M. Joyce, A. Ledovskoy, A. Li, C. Neu, B. Tannenwald, S. White, E. Wolfe

Wayne State University, Detroit, USA
N. Poudyal

University of Wisconsin - Madison, Madison, WI, USA
K. Black, T. Bose, J. Buchanan, C. Caillol, S. Dasu, I. De Bruyn, P. Everaerts, F. Fienga, C. Galloni, H. He, M. Herndon, A. Hervé, U. Hussain, A. Lanaro, A. Loeliger, R. Loveless, J. Madhusudanan Sreekala, A. Mallampalli, A. Mohammadi, D. Pinna, A. Savin, V. Shang, V. Sharma, W.H. Smith, D. Teague, S. Trembath-reichert, W. Vetens

†: Deceased
1: Also at TU Wien, Wien, Austria
2: Also at Institute of Basic and Applied Sciences, Faculty of Engineering, Arab Academy for Science, Technology and Maritime Transport, Alexandria, Egypt
3: Also at Université Libre de Bruxelles, Bruxelles, Belgium
4: Also at Universidade Estadual de Campinas, Campinas, Brazil
5: Also at Federal University of Rio Grande do Sul, Porto Alegre, Brazil
6: Also at University of Chinese Academy of Sciences, Beijing, China
7: Also at Department of Physics, Tsinghua University, Beijing, China
8: Also at UFMS, Nova Andradina, Brazil
9: Also at Nanjing Normal University Department of Physics, Nanjing, China
10: Now at The University of Iowa, Iowa City, USA
11: Also at Institute for Theoretical and Experimental Physics named by A.I. Alikhanov of NRC 'Kurchatov Institute', Moscow, Russia
12: Also at Joint Institute for Nuclear Research, Dubna, Russia
13: Also at Cairo University, Cairo, Egypt
14: Also at Purdue University, West Lafayette, USA
15: Also at Université de Haute Alsace, Mulhouse, France
16: Also at Erzincan Binali Yildirim University, Erzincan, Turkey
17: Also at CERN, European Organization for Nuclear Research, Geneva, Switzerland
18: Also at RWTH Aachen University, III. Physikalisches Institut A, Aachen, Germany
19: Also at University of Hamburg, Hamburg, Germany
20: Also at Isfahan University of Technology, Isfahan, Iran, Isfahan, Iran
21: Also at Brandenburg University of Technology, Cottbus, Germany
22: Also at Skobeltsyn Institute of Nuclear Physics, Lomonosov Moscow State University, Moscow, Russia
23: Also at Physics Department, Faculty of Science, Assiut University, Assiut, Egypt
24: Also at Karoly Robert Campus, MATE Institute of Technology, Gyongyos, Hungary
25: Also at Institute of Physics, University of Debrecen, Debrecen, Hungary
26: Also at Institute of Nuclear Research ATOMKI, Debrecen, Hungary
27: Also at MTA-ELTE Lendület CMS Particle and Nuclear Physics Group, Eötvös Loránd University, Budapest, Hungary
28: Also at Wigner Research Centre for Physics, Budapest, Hungary
29: Also at IIT Bhubaneswar, Bhubaneswar, India
30: Also at Institute of Physics, Bhubaneswar, India
31: Also at G.H.G. Khalsa College, Punjab, India
32: Also at Shoolini University, Solan, India
33: Also at University of Hyderabad, Hyderabad, India
34: Also at University of Visva-Bharati, Santiniketan, India
35: Also at Indian Institute of Technology (IIT), Mumbai, India
36: Also at Deutsches Elektronen-Synchrotron, Hamburg, Germany
37: Also at Sharif University of Technology, Tehran, Iran
38: Also at Department of Physics, University of Science and Technology of Mazandaran, Behshahr, Iran
39: Now at INFN Sezione di Bari [a], Università di Bari [b], Politecnico di Bari [c], Bari, Italy
40: Also at Italian National Agency for New Technologies, Energy and Sustainable Economic Development, Bologna, Italy
41: Also at Centro Siciliano di Fisica Nucleare e di Struttura Della Materia, Catania, Italy
42: Also at Università di Napoli 'Federico II', Napoli, Italy

43: Also at Consiglio Nazionale delle Ricerche - Istituto Officina dei Materiali, PERUGIA, Italy
44: Also at Riga Technical University, Riga, Latvia
45: Also at Consejo Nacional de Ciencia y Tecnología, Mexico City, Mexico
46: Also at IRFU, CEA, Université Paris-Saclay, Gif-sur-Yvette, France
47: Also at Institute for Nuclear Research, Moscow, Russia
48: Now at National Research Nuclear University 'Moscow Engineering Physics Institute' (MEPhI), Moscow, Russia
49: Also at Institute of Nuclear Physics of the Uzbekistan Academy of Sciences, Tashkent, Uzbekistan
50: Also at St. Petersburg State Polytechnical University, St. Petersburg, Russia
51: Also at University of Florida, Gainesville, USA
52: Also at Imperial College, London, United Kingdom
53: Also at P.N. Lebedev Physical Institute, Moscow, Russia
54: Also at California Institute of Technology, Pasadena, USA
55: Also at Budker Institute of Nuclear Physics, Novosibirsk, Russia
56: Also at Faculty of Physics, University of Belgrade, Belgrade, Serbia
57: Also at Trincomalee Campus, Eastern University, Sri Lanka, Nilaveli, Sri Lanka
58: Also at INFN Sezione di Pavia [a], Università di Pavia [b], Pavia, Italy
59: Also at National and Kapodistrian University of Athens, Athens, Greece
60: Also at Ecole Polytechnique Fédérale Lausanne, Lausanne, Switzerland
61: Also at Universität Zürich, Zurich, Switzerland
62: Also at Stefan Meyer Institute for Subatomic Physics, Vienna, Austria
63: Also at Laboratoire d'Annecy-le-Vieux de Physique des Particules, IN2P3-CNRS, Annecy-le-Vieux, France
64: Also at Şırnak University, Sirnak, Turkey
65: Also at Near East University, Research Center of Experimental Health Science, Nicosia, Turkey
66: Also at Konya Technical University, Konya, Turkey
67: Also at Istanbul University - Cerrahpasa, Faculty of Engineering, Istanbul, Turkey
68: Also at Piri Reis University, Istanbul, Turkey
69: Also at Adiyaman University, Adiyaman, Turkey
70: Also at Ozyegin University, Istanbul, Turkey
71: Also at Izmir Institute of Technology, Izmir, Turkey
72: Also at Necmettin Erbakan University, Konya, Turkey
73: Also at Bozok Universitetesi Rektörlügü, Yozgat, Turkey
74: Also at Marmara University, Istanbul, Turkey
75: Also at Milli Savunma University, Istanbul, Turkey
76: Also at Kafkas University, Kars, Turkey
77: Also at Istanbul Bilgi University, Istanbul, Turkey
78: Also at Hacettepe University, Ankara, Turkey
79: Also at Rutherford Appleton Laboratory, Didcot, United Kingdom
80: Also at Vrije Universiteit Brussel, Brussel, Belgium
81: Also at School of Physics and Astronomy, University of Southampton, Southampton, United Kingdom
82: Also at IPPP Durham University, Durham, United Kingdom
83: Also at Monash University, Faculty of Science, Clayton, Australia
84: Also at Università di Torino, TORINO, Italy
85: Also at Bethel University, St. Paul, Minneapolis, USA, St. Paul, USA
86: Also at Karamanoğlu Mehmetbey University, Karaman, Turkey

87: Also at Ain Shams University, Cairo, Egypt
88: Also at Bingol University, Bingol, Turkey
89: Also at Georgian Technical University, Tbilisi, Georgia
90: Also at Sinop University, Sinop, Turkey
91: Also at Erciyes University, KAYSERI, Turkey
92: Also at Texas A&M University at Qatar, Doha, Qatar
93: Also at Kyungpook National University, Daegu, Korea, Daegu, Korea